This article was downloaded by: *[Averianov, Alexander O.]*
On: *30 July 2010*
Access details: *Access Details: [subscription number 924972411]*
Publisher *Taylor & Francis*
Informa Ltd Registered in England and Wales Registered Number: 1072954 Registered office: Mortimer House, 37-41 Mortimer Street, London W1T 3JH, UK

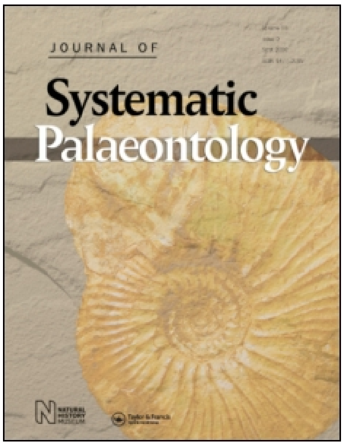

Journal of Systematic Palaeontology
Publication details, including instructions for authors and subscription information:
http://www.informaworld.com/smpp/title~content=t913521956

New material of the Late Cretaceous deltatheroidan mammal *Sulestes* from Uzbekistan and phylogenetic reassessment of the metatherian-eutherian dichotomy

Alexander O. Averianov[a]; J. David Archibald[b]; Eric G. Ekdale[c]
[a] Zoological Institute, Russian Academy of Sciences, Universitetskaya nab., Saint Petersburg, Russia [b] Department of Biology, San Diego State University, San Diego, California, USA [c] Department of Geological Sciences, The University of Texas at Austin, Austin, Texas, USA

Online publication date: 30 July 2010

To cite this Article Averianov, Alexander O. , Archibald, J. David and Ekdale, Eric G.(2010) 'New material of the Late Cretaceous deltatheroidan mammal *Sulestes* from Uzbekistan and phylogenetic reassessment of the metatherian-eutherian dichotomy', Journal of Systematic Palaeontology, 8: 3, 301 — 330

To link to this Article: DOI: 10.1080/14772011003603499

URL: http://dx.doi.org/10.1080/14772011003603499

PLEASE SCROLL DOWN FOR ARTICLE

Full terms and conditions of use: http://www.informaworld.com/terms-and-conditions-of-access.pdf

This article may be used for research, teaching and private study purposes. Any substantial or systematic reproduction, re-distribution, re-selling, loan or sub-licensing, systematic supply or distribution in any form to anyone is expressly forbidden.

The publisher does not give any warranty express or implied or make any representation that the contents will be complete or accurate or up to date. The accuracy of any instructions, formulae and drug doses should be independently verified with primary sources. The publisher shall not be liable for any loss, actions, claims, proceedings, demand or costs or damages whatsoever or howsoever caused arising directly or indirectly in connection with or arising out of the use of this material.

Journal of Systematic Palaeontology, Vol. 8, Issue 3, September 2010, 301–330

New material of the Late Cretaceous deltatheroidan mammal *Sulestes* from Uzbekistan and phylogenetic reassessment of the metatherian-eutherian dichotomy

Alexander O. Averianov[a]*, J. David Archibald[b] and Eric G. Ekdale[c]

[a]*Zoological Institute, Russian Academy of Sciences, Universitetskaya nab., Saint Petersburg 199034, Russia;* [b]*Department of Biology, San Diego State University, San Diego, California 92182-4614, USA;* [c]*Department of Geological Sciences, The University of Texas at Austin, One University Station C-114, Austin, Texas 78712, USA*

(Received 7 July 2009; accepted 8 December 2009)

Sulestes karakshi Nessov, 1985b (= *Deltatheroides kizylkumensis* Nessov, 1993 = *Marsasia aenigma* Nessov, 1997) from the Late Cretaceous (Turonian) Bissekty local fauna, Kyzylkum Desert, Uzbekistan, is revised based on additional material from the type locality. It is characterized by an absence of palatal vacuities, double-rooted P1, an asymmetrical M3 with reduced metastylar lobe, an unreduced M4 and m4, obliquely oriented p1, anterior wall of the upper canine alveolus formed by premaxilla, and Meckelian groove on the dentary. PAUP analyses using a data matrix modified from Rougier *et al*. (1998, 2004) places *Sulestes* within Deltatheridiidae in an unresolved trichotomy with the Mongolian Campanian *Deltatheridium* and *Deltatheroides*. *Oklatheridium* from the Early Cretaceous of North America is sister taxon to these Late Cretaceous Asiatic deltatheridiidans. Deltatheridiidae is the sister group to other Metatheria including the crown clade Marsupialia. A *Deltatheroides*-like taxon from the Maastrichtian at Guriliin Tsav, Mongolia, is not related to the Stagodontidae but is sister taxon to other Boreometatheria. The North American Early Cretaceous *Atokatheridium*, *Pappotherium*, and *Montanalestes* are stem tribosphenic mammals, while *Holoclemensia* is at the base of the eutherian lineage.

Keywords: Metatheria; Eutheria; phylogeny; evolution; Mesozoic; Asia

Introduction

Deltatheroida is a clade of basal metatherian mammals from the Late Cretaceous of Asia and possibly Early and Late Cretaceous of North America (Gregory & Simpson 1926; Van Valen 1966, 1974; McKenna *et al*. 1971; Szalay & McKenna 1971; Butler & Kielan-Jaworowska 1973; Fox 1974; Kielan-Jaworowska 1975; Kielan-Jaworowska *et al*. 1979, 2000, 2004; Cifelli 1990, 1993bb; Kielan-Jaworowska & Nessov 1990; Averianov 1997; Rougier *et al*. 1998, 2004; Horovitz 2000; Wood 2000; Kielan-Jaworowska & Cifelli 2001; Averianov & Archibald 2003; Davis *et al*. 2008).

In the Late Cretaceous of the Kyzylkum Desert, Uzbekistan, a succession of three relatively well-described mammalian faunas, all dominated by eutherian mammals, is known: the early Cenomanian Sheikhdzheili local fauna, the middle-late Turonian Bissekty local fauna, and the late Turonian-?Coniacian Aitym local fauna (see Archibald & Averianov 2005 for review and further references). Nevertheless, a number of specimens from these faunas have been attributed to various metatherian taxa.

The first metatherian specimens reported from the region were a canine (CCMGE 5/11758; Nessov 1981, fig. 9(22), 1982, pl. 1, fig. 8; Nessov & Kielan-Jaworowska 1991, fig. 1) and a juvenile dentary fragment with alveoli for m2-4 (CCMGE 16/11758; Nessov 1982, pl. 2, fig. 7) from the Bissekty local fauna at Dzharakuduk referred to Deltatheridiidae. The attribution of both of these specimens to Deltatheridiidae is confirmed by this study.

The first metatherian taxon established from the Bissekty local fauna was *Sulestes karakshi* Nessov, 1985b, based on a maxillary fragment with M1-2 (CCMGE 35/12000) and attributed to a new subfamily Sulestinae Nessov, 1985b within Deltatheridiidae. Nessov (1987) figured and Kielan-Jaworowska & Nessov (1990) figured and described a dentary fragment with m1 (CCMGE 5/12455, identified here as m2) referred to as *Sulestes* sp. Subsequently Nessov described a second metatherian taxon from the Bissekty local fauna, *Delatheroides kizylkumensis* Nessov, 1993, based on two isolated lower molars (CCMGE 40/12455 and 41/12455). This species was later made the type of the new genus *Deltatherus* Nessov, 1997. The third metatherian taxon described from the Bissekty local fauna was *Marsasia aenigma* Nessov, 1997, based on two edentulous dentary fragments (ZIN 82620 and 83130) and originally referred to Marsupialia. Averianov & Kielan-Jaworowska (1999) restudied these specimens, confirmed their attribution to the Marsupialia, and indicated that *Marsasia* might be referable to the endemic Asiatic marsupial order

---

*Corresponding author. Email: dzharakuduk@mail.ru.

ISSN 1477-2019 print / 1478-0941 online

DOI: 10.1080/14772011003603499
http://www.informaworld.com

Asiadelphia. These authors also described a dentary fragment with the last molar (ZIN 83131) and classified this specimen as *Marsasia* sp. Finally, Averianov & Archibald (2003) identified an incomplete upper molar (ZIN 85049) from the Aitym local fauna as *Deltatherus* sp.

Oxlestes grandis Nessov, 1982, based on a large axis (CCMGE 6/11758) from the Sheikhdzheili local fauna, has been assigned, sometimes with reservation, to Deltatheroida by various authors (Nessov *et al*. 1994; McKenna & Bell 1997; Nessov 1997; Averianov 2000; Kielan-Jaworowska *et al*. 2004). This assignment was questioned by others (e.g. Rougier *et al*. 2004). Averianov & Archibald (2005) considered this specimen as possibly belonging to a large, currently undetermined zhelestid known from the Sheikhdzheili local fauna.

Our investigation of the metatherian specimens from the Bissekty local fauna reveals that only one metatherian taxon, *Sulestes karakshi*, is present, with *Deltatherus kizylkumensis* and *Marsasia aenigma* being synonyms and *Marsasia* sp. being attributable to the eutherian *Paranyctoides aralensis* Nessov, 1993 (Archibald & Averianov 2005).

In this report we present results of a detailed study of all available non-postcranial metatherian specimens from the Bissekty local fauna collected between 1978 and 2006 by L. Nessov's and international URBAC expeditions.

Methods

For osteological terminology we follow Wible (2003), except in two cases: we use "dentary" instead of "mandible" and "palatal vacuity" instead of "major palatine foramen". The classification of Mesozoic mammals proposed by Kielan-Jaworowska *et al*. (2004) is generally adopted here. Wear facet nomenclature is after Crompton (1971). Mongolian place names and stratigraphic terms are transliterated according to Benton (2000). Measurements of teeth were taken according to the method illustrated by Archibald (1982, fig. 1). Teeth were measured using an ocular scale of a Leica MZ6 binocular microscope. Photographs were taken with a Canon PowerShot S60 digital camera mounted on a Leica MZ6 binocular microscope through a Canon conversion lens adapter LA-DC100. The methods of the phylogenetic analysis are explained in the relevant section.

Measurements

AW = anterior width
L = length
PW = posterior width
TAL = talonid length
TAW = talonid width
TRA = trigonid angle
TRL = trigonid length
TRW = trigonid width
W = width

All measurements (except angles) are in mm.

Material

Institutional Abbreviations

AMNH: American Museum of Natural History, New York; **CCMGE**: Chernyshev's Central Museum of Geological Exploration, Saint Petersburg; **CNHM**: Field Museum of Natural History, Chicago; **OMNH**: Oklahoma Museum of Natural History, Oklahoma; **SMP-SMU**: Shuler Museum of Palaeontology, Southern Methodist University, Dallas; **URBAC**: Uzbek/Russian/British/American/Canadian Joint Palaeontological Expedition specimens currently at San Diego State University, San Diego; **ZIN**: Zoological Institute, Russian Academy of Sciences, Saint Petersburg; **ZPAL**: Institute of Palaeobiology, Polish Academy of Sciences, Warsaw.

Locality Indexes

CBI: Central [Kyzylkum Desert], Bissekty Formation, locality index used by L. Nessov for localities within the middle and upper parts of the Bissekty Formation; **CDZH**: Central [Kyzylkum Desert], Dzharakuduk, locality index used by L. Nessov for localities within the lower part of the Bissekty Formation.

Systematic palaeontology

Mammalia Linnaeus, 1758
Tribosphenida McKenna, 1975
Metatheria Huxley, 1880
Deltatheroida Kielan-Jaworowska, 1982
Deltatheridiidae Gregory & Simpson, 1926

1926 Deltatheridiidae Gregory & Simpson: 6.
1971 Deltatheridiidae Szalay & McKenna: 286.
1975 Deltatheridiidae Kielan-Jaworowska: 107.
1985b Sulestinae Nessov: 210.
1990 Deltatheridiidae Kielan-Jaworowska & Nessov: 2.
1990 Deltatheroididae Kielan-Jaworowska & Nessov: 2.
2004 Deltatheridiidae Kielan-Jaworowska *et al*.: 445.

Type genus. *Deltatheridium* Gregory & Simpson, 1926.

Diagnosis. See Kielan-Jaworowska *et al*. (2004: 445).

Included genera. Type genus, *Oklatheridium* Davis, Cifelli & Kielan-Jaworowska, 2008, *Sulestes* Nessov, 1985b, and *Deltatheroides* Gregory & Simpson, 1926.

Definition. The last common ancestor of *Oklatheridium*, *Deltatheridium*, *Sulestes*, and *Deltatheroides* and all of its descendants.

Remarks. The original concept of Deltatherididae was based on three genera from the Late Cretaceous (Campanian) of the Gobi Desert, Mongolia: *Deltatheridium*, *Deltatheroides* and *Hyotheridium* (Gregory & Simpson, 1926). Taxonomic affinities of these taxa have long been debated (see Kielan-Jaworowska *et al.* 2004 for review). The current consensus is that *Deltatheridium* and *Deltatheroides* are metatherians while *Hyotheridium* might be a eutherian (Kielan-Jaworowska & Nessov, 1990; Rougier *et al.* 1998, 2004; Kielan-Jaworowska *et al.* 2000, 2004). Kielan-Jaworowska & Nessov (1990) proposed a new classification for deltatheroidans, divided into Deltatherididae (*Deltatheridium* and *Sulestes*) and Deltatheroididae (*Deltatheroides* and the unnamed Guriliin Tsav taxon from the Maastrichtian of Mongolia). Deltatherididae were characterized by small size, lack of palatal vacuities, three upper molars, and m4 with reduced talonid. Deltatheroididae are larger animals with palatal vacuities and M4/m4 not reduced. Among these characters, the indication of three upper molars for Deltatherididae is invalid because M4 is present in both *Deltatheridium* and *Sulestes* (Rougier *et al.* 1998; this report). This classification was followed by McKenna & Bell (1997) and Averianov & Archibald (2003) but not by Kielan-Jaworowska *et al.* (2000), who in particular doubted the presence of palatal vacuities in the holotype of *Deltatheroides cretacicus* Gregory & Simpson, 1926 (AMNH 21700).

A further modification to deltatheroidan classification was proposed by Rougier *et al.* (1998, fig. 5), who grouped the unnamed Guriliin Tsav taxon with the North American Stagodontidae, although this grouping collapsed in slightly longer trees (see also Wible *et al.* 2001; Rougier *et al.* 2004). The molars of the unnamed Guriliin Tsav taxon, as well as other deltatheroidans (see Van Valen 1974), are indeed similar to those of the North American stagodontids (Clemens 1966; Fox & Naylor 2006). In our analysis this hypothesis is rejected and the unnamed Guriliin Tsav taxon is a sister taxon to later branching Boreometatheria (see below). Davis *et al.* (2008) expanded Deltatherididae to include *Atokatheridium* and *Oklatheridium* from the Early Cretaceous of North America. According to our analysis, the monophyletic Deltatherididae includes four taxa (*Oklatheridium*, *Deltatheridium*, *Deltatheroides*, and *Sulestes*), while *Atokatheridium* is a stem tribosphenidan (see below).

Several taxa based on isolated teeth from the Late Cretaceous of North America (Fox 1974; Cifelli 1990; Rougier *et al.* 2004) might also belong to Deltatherididae.

Genus ***Sulestes*** Nessov, 1985b

1985b *Sulestes* Nessov: 211.
1994 *Sulestes* Nessov *et al.*: 65.
1997 *Deltatherus* Nessov: 163.
1997 *Marsasia* Nessov: 164.
1999 *Marsasia* Averianov & Kielan-Jaworowska: 72.
2004 *Sulestes* Kielan-Jaworowska *et al.*: 446.
2004 *Deltatherus* Kielan-Jaworowska *et al.*: 446.
2004 *Marsasia* Kielan-Jaworowska *et al.*: 451.

Type and only known species. *Sulestes karakshi* Nessov, 1985b.

Diagnosis. As for type and only species.

Distribution. Uzbekistan, Late Cretaceous (Turonian).

Sulestes karakshi Nessov, 1985b
(Figs 1–5, 7)

1981 Deltatherididae Nessov: fig. 9(22).
1982 Deltatherididae Nessov: pl. 1, fig. 8, pl. 2, fig. 7.
1985a Theria Nessov: 16, pl. 2, fig. 5.
1985a *Sulestes karakshy* [sic, nomen nudum] Nessov: 14, pl. 3, fig. 15.
1985b *Sulestes karakshi* Nessov: 211, pl. 2, fig. 1.
1987 *Sulestes* sp. Nessov: pl. 1, fig. 5.
1990 *Sulestes karakshi* Kielan-Jaworowska & Nessov: figs 3, 4A.
1990 *Sulestes* sp. Kielan-Jaworowska & Nessov: 3, figs 1, 2A-E.
1991 *Sulestes karakshi* Nessov & Kielan-Jaworowska: fig. 1.
1993 Deltatheridae [sic] Nessov: fig. 2(2).
1993 *Deltatheroides kizylkumensis* Nessov: 122, fig. 4(1, 2).
1994 *Sulestes karakshi* Nessov *et al.*: pl. 4, fig. 3.
1997 *Sulestes karakshi* Nessov: pl. 45, fig. 5, pl. 46, fig. 5.
1997 *Sulestes* sp. Nessov: pl. 45, fig. 6.
1997 Deltatheroida indet. Nessov: pl. 46, fig. 4.
1997 [Mammalia indet.] Nessov: pl. 47, fig. 4.
1997 *Deltatherus kizylkumensis* Nessov: 163, pl. 45, figs 2–4.
1997 *Marsasia aenigma* Nessov: 164, pl. 47, figs 1, 2.
1999 *Marsasia aenigma* Averianov & Kielan-Jaworowska: 73, figs 1, 2.
2000 *Sulestes karakshi* Averianov: 640, fig. 30.5K.
2000 *Sulestes* sp. Averianov: 640, fig. 30.6M, N.
2000 ‘*Delatheroides*’ *kizylkumensis* Averianov: 640.
2000 [Mammalia indet.] Averianov: fig. 30.5L, M.
2000 *Delatheroides kisylkumensis* [sic] Averianov: fig. 30.6E.

2000 *Delatheroides kizylkumensis* [possible] Averianov: fig. 30.6F.
2004 *Sulestes karakshi* Kielan-Jaworowska *et al*.: 446, fig. 12.7B1.
2004 *Sulestes* sp. Kielan-Jaworowska *et al*.: fig. 12.7B2, 3.
2004 *Deltatherus kizylkumensis* Kielan-Jaworowska *et al*.: 446, fig. 12.7C.
2004 *Marsasia aenigma* Kielan-Jaworowska *et al*.: 452, fig. 12.9B.
2004 *Sulestes karakshi* Rougier *et al*.: fig. 6D.
2005 *Sulestes karakshi* Archibald & Averianov: figs 2L, 3E.
2008 *Sulestes karakshi* Davis *et al*.: fig. 1.8E.

Holotype. CCMGE 35/12000, left maxilla fragment with M1-2 and alveoli for P3 and M3. Collected by Lev A. Nessov, 7 September, 1980.

Type locality and horizon. CBI-4b site, Dzharakuduk locality, Itemir-Dzharakuduk Depression, central Kyzylkum Desert, Navoi Viloyat, Uzbekistan. Bissekty Formation (Upper Cretaceous: Turonian).

Revised differential diagnosis. Differs from both *Deltatheridium* and *Deltatheroides* by p1 oriented obliquely relative to the dentary axis. Plesiomorphically similar to *Deltatheridium* and differs from *Deltatheroides* in having an asymmetrical M3 with reduced metastylar lobe. Plesiomorphically similar to *Deltatheroides* and differs from *Deltatheridium* in having M4/m4 not vestigial, m4 with metaconid and three-cusped basined talonid. Differs plesiomorphically from both *Deltatheridium* and *Deltatheroides* in having Meckelian groove present at least in some specimens. Differs from *Deltatheridium* in having P1 double rooted and premaxilla overlapping laterally anterior end of maxilla and forming anterior wall of upper canine alveolus (these characters are not known for *Deltatheroides*; the first character is plesiomorphic, for the second character see comments below). Differs from *Oklatheridium* by larger size, smaller stylocone, shallower ectoflexus, and more open trigonid.

Remarks. Nessov's original diagnosis of *Sulestes* (Nessov 1985b, p. 211), translated into English in Nessov *et al.* (1994, p. 65), contains a number of minor details that are either shared with *Deltatheridium* or are highly variable in the presently known sample, such as enamel crenulations along the ectocingulum or paracingulum (see description below). At least one character mentioned in that diagnosis, a somewhat wider paracingulum on upper molars compared with *Deltatheridium* (and *Deltatheroides*), might be potentially important. Another potentially diagnostic character might be the presence of slightly better developed conules and internal conular cristae on upper molars in *Sulestes* compared with the Mongolian deltatheroidans. But as these structures vary in the known sample of *Sulestes* and their development in the Mongolian specimens might be obscured by poorer preservation, we follow Rougier *et al.* (1998, 2004) in considering all three deltatheroidan taxa as having the same states for these two characters: paracingulum (= preparacingulum of those authors) continuous and conules small, without cristae.

Another common character of *Sulestes* and *Deltatheridium*, differentiating both taxa from *Deltatheroides*, might be the lack of the palatal vacuities, which likely were present in *Deltatheroides* (see comments for Deltatheridiidae above).

The dentary and lower dental characters for *Deltatheroides* are based upon ZPAL MgM-I/29 from the Djadokhta Formation at the Bayan Zag (= Bayn Dzak) locality in the Gobi Desert, Mongolia (Kielan-Jaworowska 1975, pl. 35, fig.1).

In the unnamed Guriliin Tsav taxon from the Maastrichtian of Mongolia, the metatherians *Mayulestes* Muizon, 1994 and *Szalinia* Muizon & Cifelli, 2001 from the Paleocene of South America, in borhyaenids, and in some extant marsupials (e.g. Phalangeridae, Phascolarctidae, Pseudocheiridae) the lateral margin of the paracanine fossa is formed by premaxilla and maxilla (character 81[1] of Rougier *et al*. (1998, 2004) and Wible *et al*. (2001)) and the premaxilla participates in the upper canine alveolus. In *Sulestes* the premaxilla is not known, but judging from its suture preserved on the maxilla (see description) it undoubtedly formed the anterior margin of the canine alveolus; and thus such a peculiar construction of the paracanine fossa was also characteristic for *Sulestes*.

Referred specimens. URBAC 03-150, right petrosal (CBI-14); CCMGE 40/12000, right maxilla with alveoli for C, P1-3, and M1-3 (CBI-14, 1989); CCMGE 5/11758, right C (CDZH-17a, 1978); URBAC 04-164, left maxilla fragment with DP3, M1, alveoli for P1-2, and crown of erupting P3 (CBI-14); ZIN 90312, left maxilla fragment with alveoli for P3 and M1-4 (CBI-14, 1984); URBAC 04-149, left maxilla fragment with M2-3 and alveoli for M1 and M4 (CBI-14); URBAC 04-345, right M1 lacking parastylar region (CBI-17); URBAC 99-017, left M2 (CBI-14); URBAC 00-057, right dentary fragment with broken c, p3, alveoli for i1-3, p1, m1, and roots of p2 (CBI-14); URBAC 06-005, right dentary fragment with m1, 2, 4, alveoli for c, p1-3, m3, and base of angular, condylar, and coronoid processes (CBI-17); URBAC 03-043, right dentary fragment with alveoli for c, p1-3, m1-4, and bases of angular, condylar, and coronoid processes (CBI-14); ZIN 89008, left dentary fragment with alveoli for c, p1-3, and m1-4 (CBI-14, 1980); URBAC 03-184, right dentary fragment consisting of two pieces lacking contact, anterior, with alveoli for c, p1–3, and m1–2, and posterior, with bases of the angular, condylar, and coronoid processes (CBI-4e); ZIN 88467, right dentary fragment with alveoli for c, p1-3, and m1-3 (CBI-14); ZIN 88486, right dentary fragment with alveoli for c, p1-3, and m1-2 (CBI-4b, 1980); ZIN 90310, right dentary fragment with alveoli for c, p1-3, and m1-2 (CBI-14, 1989); ZIN 89007, right dentary fragment with m3 missing most of the trigonid, alveoli for p1-3, m1, 2, and 4, and base of the coronoid process (CBI-5a, 1989); ZIN 82620, left dentary fragment with alveoli for p1-3, m1-4, bases of angular and condylar processes and most of the coronoid process (CBI-51, 1989; holotype of *Marsasia aenigma* Nessov, 1997); URBAC 03-222, right dentary with alveoli for p3 and m1-4 and base of the coronoid process (CBI-14); ZIN 90311, right dentary fragment with alveoli for p3 and m1-3 (CBI-14, 1980); CCMGE 5/12455, left dentary fragment with m1 talonid and m2 heavily worn (CBI-14, 1984); ZIN 88130, right dentary fragment with alveoli for m2-4, base of angular process, and condylar and coronoid processes (CBI-4b); URBAC 06-006, right dentary process with alveoli for m2-4, base of the angular process, and most of the coronoid process (CBI-14); URBAC 03-104, left dentary fragment with alveoli for m2-4 and bases for the angular and coronoid processes, juvenile (CBI-14); CCMGE 16/11758, right dentary fragment with alveoli for m2-4 and base of the coronoid process, juvenile (CBI-4v, 1979); URBAC 03-090, left dentary fragment with alveoli for m3-4, base of the angular process and most of the coronoid process (CBI-14); URBAC 02-023, right dentary fragment with alveoli for m3-4 and bases of angular and coronoid processes, juvenile (CBI-4e); ZIN 90309, left dentary fragment with alveoli for m3-4 and base of the coronoid process (CBI-14, 1989); URBAC 02-111, left m1 (CBI-4e); URBAC 00-001, left m2 (CBI-14); URBAC 03-009, left m2 (CBI-14); URBAC 03-194, left m2 (CBI-4e); URBAC 04-344, left m2 (CBI-14); URBAC 04-291, right m2 trigonid (CBI-14); CCMGE 40/12455, left m3 (CBI-4, 1989; holotype of *Deltatheroides kizylkumensis* Nessov, 1993; in Nessov (1993, 1997) the locality for this specimen is incorrectly indicated as CBI-14); CCMGE 41/12455, left m3 heavily worn (CBI-51, 1989; in Nessov (1993, 1997) the locality for this specimen is incorrectly indicated as CBI-14); URBAC 98–012, right m3 heavily worn (CBI-14); URBAC 02-093, left m3 heavily worn (CBI-4e); URBAC 06-019, right m3 trigonid heavily worn (CBI-14); URBAC 04-169, right m3 (CBI-14); URBAC 04-217, left m4 (CBI-14); URBAC 04-346, left m4 (CBI-14).

Description of *Sulestes karakshi*

Maxilla

The maxilla is known from several specimens, the most nearly complete of which is CCMGE 42/12000 (Fig. 1A–C). The facial process of the maxilla is not completely preserved on any specimen. A prominent facet for the jugal is along the posterolateral edge of the maxilla, which can be seen from the lateral side as a deep and gently curved strap-like depression bordered anteriorly and ventrally by a distinct ridge (Figs 1A, 2D). The jugal facet is best preserved in CCMGE 35/12000 (holotype, not figured here), where its anterodorsal point could represent the lacrimal facet. The jugal facet extends anteriorly toward the level between the P3 roots; posteriorly, it occupies the entire lateral surface of a short zygomatic process. The ventral margin of the infraorbital foramen is preserved only in CCMGE 42/12000, where its posterior margin is above the anterior root of P3 (Fig. 1A). The infraorbital foramen is relatively small, about 1 mm in mediolateral width, oval, and faces anteriorly. A very large, subcircular depression with a distinct ventral rim placed anterior to the opening of the infraorbital canal and close to the alveolar border. This depression extends anteriorly onto the lateral wall of the canine alveolus (Fig. 1A). The internal surface of the canine alveolus is covered by characteristic grooves of varying depths that are parallel to the long axis of the canine (Fig. 1A); such grooves are not present or very weak and few in alveoli for other teeth in the maxilla. A flattened triangular area tapering anteriorly toward the end of the maxilla can be seen in lateral view just anterior to the canine alveolus (Fig. 1A). This area is possibly the facet for the premaxilla. If this interpretation is correct, the premaxilla overlapped the anterior end of the maxilla laterally and formed the anterior wall of the canine alveolus, as in some modern diprotodontians. But in contrast to modern didelphids, in which the anterior wall of the canine alveolus is formed by the maxilla and a short anterior process of the maxilla overlaps laterally the posterior end of the premaxilla (Wible 2003).

In CCMGE 42/12000 the palatal process of the maxilla is preserved for most of its length but is broken posteriorly at the level between M1 and M2 (Fig. 1B). The intermaxillary suture is straight, thicker anteriorly than posteriorly. Its most posterior preserved end is at the level between M2 and M3. The bone is very thin here and the intermaxillary suture possibly did not extend posteriorly beyond the distal end of M2. The palatal process is widest opposite M1 ($\sim$5 mm). Its ventral surface is relatively flat, with a few small irregular pits and grooves for blood vessels. A distinct sinusoidal groove is present just lingual to the alveoli between the posterior root of P3 and the lingual root of M2 (Fig. 1B). In ZIN 90312 a similar groove is situated lingual to the M3-4 alveoli (Fig. 1D). On the anterior end of the maxilla in CCMGE 42/12000 a semicircular incision is present, possibly for the palatine process of the premaxilla (Figs 1B, C). Along the posterior margin of this fragment, at the level of M2, a suture for the palatine is incompletely preserved (Fig. 1B). Medial and lateral to this suture the bone is broken and thus the broken margin cannot be interpreted as a margin for a palatal vacuity. This, together with absence of a longitudinal groove on the maxilla usually associated with such a vacuity, suggests that palatal vacuities were not present in *Sulestes*.

The canine alveolus is the largest in the maxilla (Fig. 1A, B). Its length is roughly equal to the combined length of

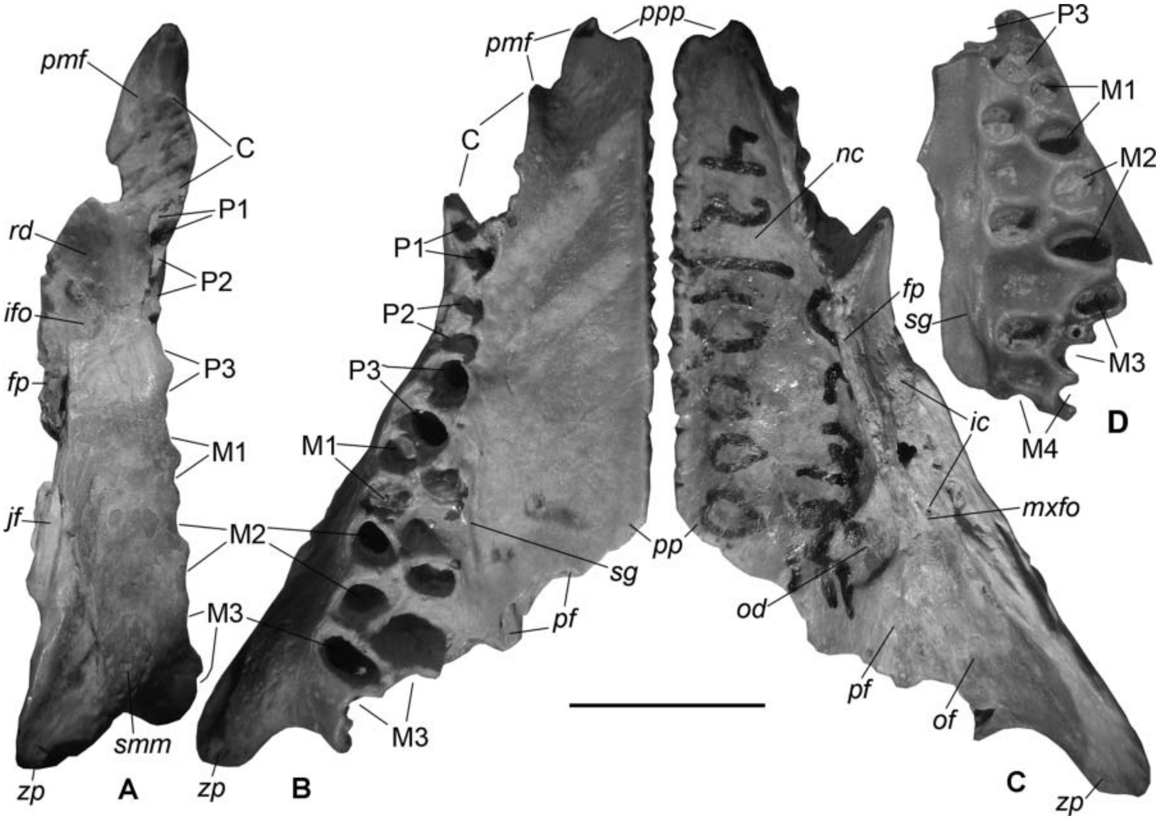

Figure 1. Edentulous maxillary fragments of *Sulestes karakshi* Nessov, 1985b from the Turonian Bissekty Formation of Dzharakuduk, central Kyzylkum Desert, Uzbekistan. **A-C,** CCMGE 42/12000, fragment of a right maxilla with alveoli for C, P1-3, and M1-3, in lateral **(A)**, ventral **(B)**, and dorsal **(C)** views; **D,** ZIN 90312, fragment of a left maxilla with alveoli for P3 and M1-4 in ventral view. Scale bar equals 5 mm. Abbreviations: fp, facial process; ic, infraorbital canal; ifo, infraorbital foramen; jf, jugal facet; mxfo, maxillary foramen; nc, nasal cavity; od, oval depression; of, orbital floor; pf, palatine facet; pmf, premaxilla facet; pp, palatal process; ppp, palatine process of premaxilla; rd, round depression; smm, superficial masseter muscle attachment area; sg, sinusoid groove; zp, zygomatic process.

the alveoli for P1-2. The alveoli for P1 and P2 are similar in size and that for P3 is distinctly larger. In all upper premolars the anterior alveolus is somewhat smaller than the posterior alveolus. The alveoli for P2 are parallel to the intermaxillary suture, and those for P1 and P3 are obliquely set in the tooth row: in P1 the anterior root is more labial while in P3 the posterior root is more labial. This gives an arcuate appearance for the upper premolar alveolar series in palatal view (Fig. 1B).

The molar alveoli gradually increase in size from M1 to M3 and then abruptly decrease for M4 (Figs 1B, 1D, 2C). The edentulous maxillary fragments of *Sulestes* are easily distinguishable in that the alveoli for the lingual molar roots are roughly equal to the alveoli for labial roots (Figs 1B, D), whereas in the contemporaneous eutherians from Dzharakuduk the lingual molar roots are much larger than the labial roots. The symmetrical M1-2 lingual and mesiolabial alveoli are rounded and similar in size, whereas the distolabial alveolus is mesiodistally compressed and longer labiolingually. In the asymmetrical M3 the situation is opposite: the mesiolabial alveolus is mesiodistally compressed and longer labiolingually, and the distolabial alveolus is rounded and similar in size to the lingual alveolus (Fig. 1D). The M4 alveoli, partially preserved in ZIN 90312 and URBAC 04-149 (Figs 1D, 2C), are a reduced copy of the M3 alveoli. The lingual margins of the alveoli for all molars, including M4, are set on the same line (Figs 1B, D), as in modern didelphids. In *Deltatheridium*, a smaller M4 is labiolingually centred on M3 (Rougier *et al*. 1998, fig. 1a, and contra description by these authors on p. 459 that “M4 is positioned lingually to the metacone of M3”; see also Rougier *et al*. 2004, fig. 6B). Between the alveoli for the lingual roots of the upper molars there are embrasure pits for reception of the corresponding lower molar trigonids; the largest depression is between the alveoli for M2 and M3 for the trigonid of m3 (Figs 1B, D).

The zygomatic process of the maxilla is short, with the posterior end approximately opposite to M4 and the anterior edge very gradually sloping towards the level between P3 and M1 (Figs 1A–C, 2C, D). The posterior edge of the

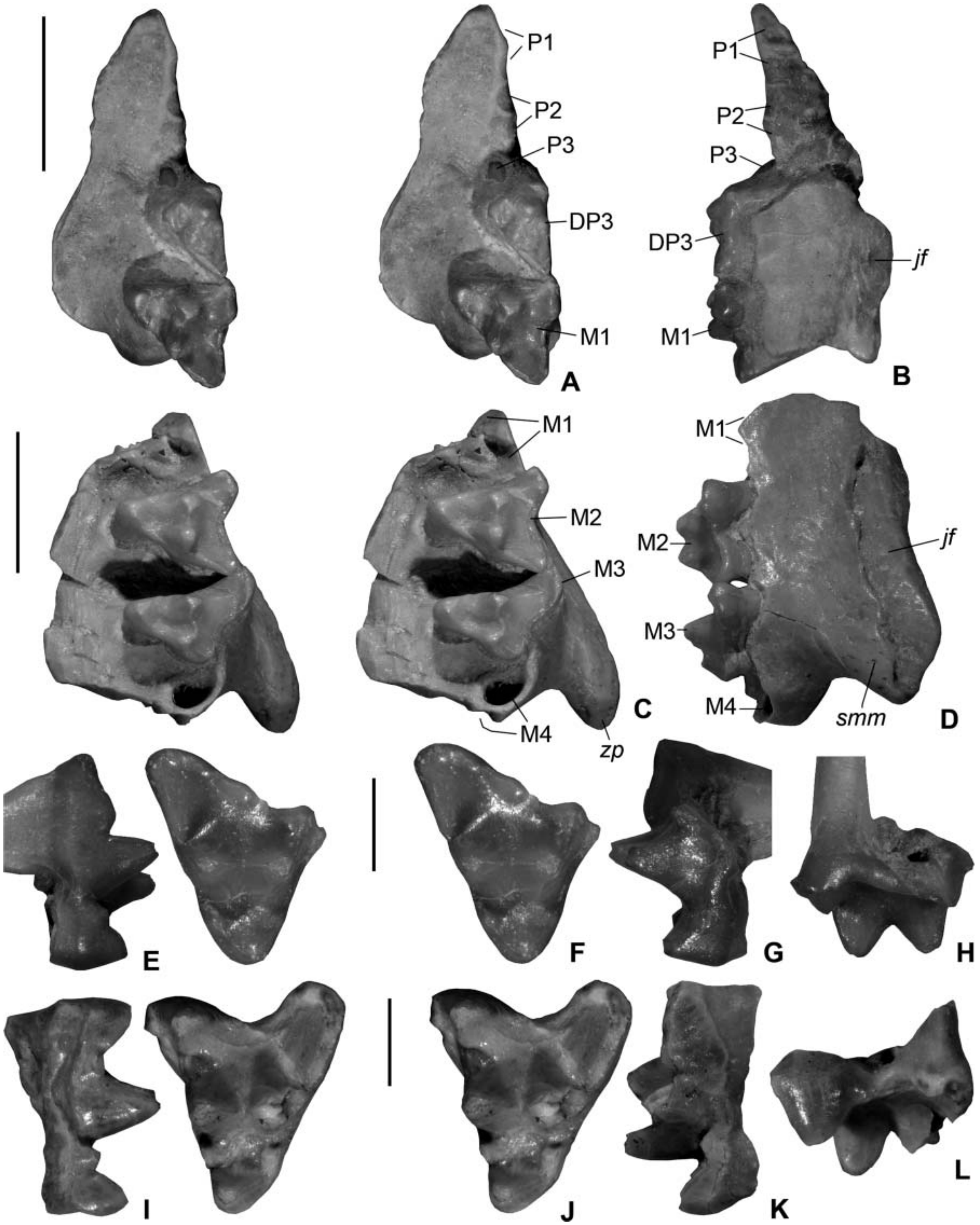

Figure 2. Maxillary fragments with dentition and isolated upper molars of *Sulestes karakshi* Nessov, 1985b from the Turonian Bissekty Formation of Dzharakuduk, central Kyzylkum Desert, Uzbekistan. **A, B,** URBAC 04-164, fragment of a left maxilla with DP3, M1, erupting crown of P3, and alveoli for P1, 2, in occlusal (**A**, stereopair) and lateral (**B**) views; **C, D,** URBAC 04-149, fragment of a left maxilla with M2, 3 and alveoli for M1, 4, in occlusal (**C**, stereopair) and lateral (**D**) views; **E-H,** URBAC 04–345, right M1 missing the parastylar lobe, in distal (**E**), occlusal (**F**, stereopair), mesial (**G**), and labial (**H**) views; **I-L**, URBAC 99-017, left M2, in mesial (**I**), occlusal (**J**, stereopair), distal (**K**), and labial (**L**) views. Scale bar equals 3 mm (**A-D**) and 1 mm (**E-L**). Abbreviations: jf, jugal facet; smm, superficial masseter muscle attachment area; zp, zygomatic process.

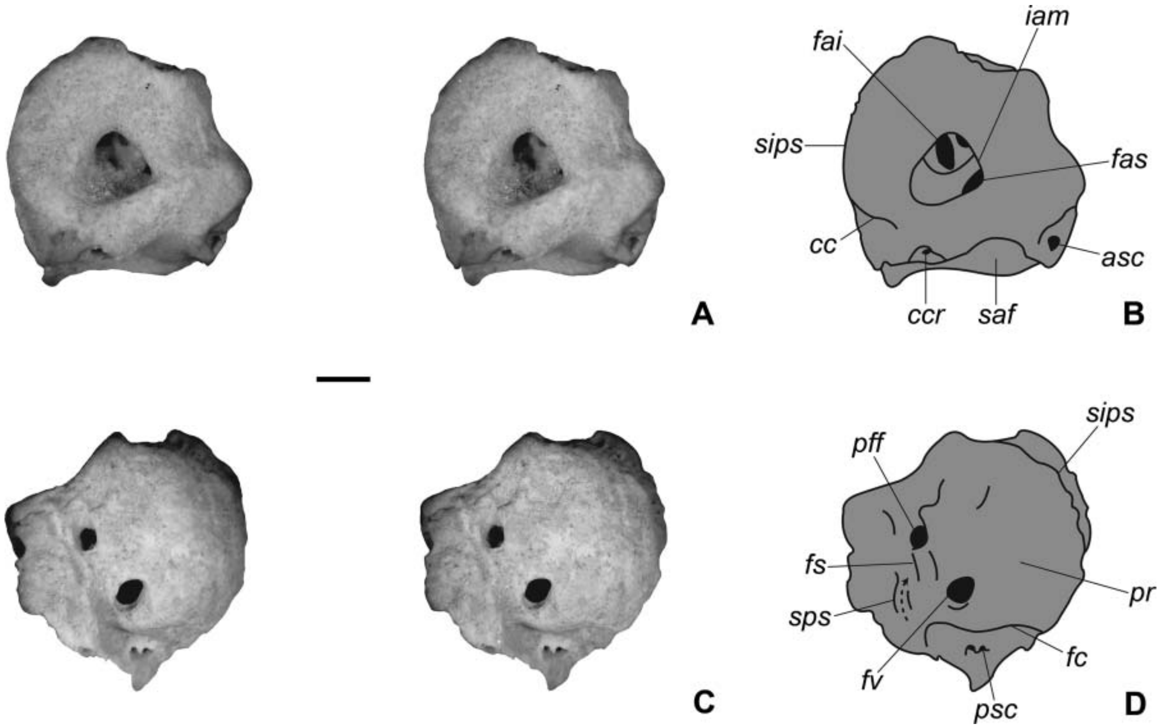

Figure 3. Right petrosal of *Sulestes karakshi* Nessov, 1985, URBAC 03-150, from the Turonian Bissekty Formation of Dzharakuduk, central Kyzylkum Desert, Uzbekistan, in cerebellar view (**A,** stereopair, lateral towards right; **B,** explanatory drawing**)** and in tympanic view (**C,** stereopair, lateral towards left; **D,** explanatory drawing). Scale bar equals 1 mm. Abbreviations: asc, anterior semicircular canal; cc, canaliculus cochlearis; ccr, crus commune; fai, foramen acusticum inferius; fas, foramen acusticum superius; fc, fenestra cochleae; fs, sulcus for facial nerve; fv, fenestra vestibuli; iam, internal auditory meatus; pff, primary facial foramen; pr, promontorium; psc, posterior semicircular canal; saf, subarcuate fossa; sips, sulcus for inferior petrosal sinus; sps, sulcus for prootic sinus. Dashed arrow indicates path of prootic sinus.

maxilla is deeply incised between the zygomatic process and alveolar border. A marked rugosity for attachment of the superficial masseter muscle is present on the lateral side of the zygomatic process, just ventral to the jugal suture and above the alveoli for M3-4 (Figs 1A, 2B; compare with Hiiemae & Jenkins 1969, fig. 4A).

The dorsal surface of the maxilla is subdivided into a larger anteromedial portion, forming the flat and smooth ventral floor of the nasal cavity, and a smaller posterolateral portion, forming the concave ventral floor of the orbit (Fig. 1C). The orbital floor is an anteriorly pointed triangular area bordered laterally by the zygomatic process and medially by a poorly discernable contact line with the palatine. The anterior end of the orbital floor forms the ventral margin of a poorly defined maxillary foramen and continues anteriorly into a rather short infraorbital canal (Fig. 1C). Anterior to the maxillary foramen the medial side of the infraorbital canal is formed by the facial process of maxilla. A shallow, oval depression is posteromedial to the maxillary foramen in CCMGE 42/12000 and ZIN 90312 (Fig. 1C). The dorsal surface of the maxilla that contributes to the floor of the orbit is covered by several pits for blood vessels of varied sizes. This part of the maxilla contains molar roots that are not exposed on the bone surface.

Petrosal

A single, isolated petrosal is attributable to *Sulestes* (URBAC 03-150; Fig. 3). The promontorium is preserved in full, but most of the posterior part of the petrosal is missing, exposing the semicircular canals in various places.

The petrosal is identified as metatherian based on the lack of a sulcus for the stapedial artery, a low stapedial ratio (1.57; following Segall 1970), and a short and horizontal prootic canal (a state that is not observed in any eutherian). The phylogenetic characters of Rougier *et al*. (2004) were coded for URBAC 03-150. The states of characters that could be coded for the petrosal are identical as those for the petrosal of *Deltatheridium*. Because *Sulestes karakshi* is the only metatherian taxon known to be present in the Bissekty local fauna, URBAC 03-150 is attributed to this species. In fact, URBAC 03-150 appears similar to the petrosal of *Deltatheridium* (Rougier *et al*. 1998, fig. 3) in that both petrosals have a round, almost circular, promontorium, and they both lack a hiatus Fallopii.

The internal auditory meatus is located at the anterior aspect of the cerebellar surface of the petrosal (Fig. 3A, B). The dorsal rim of the meatus is triangular with rounded corners. The meatus itself is deep, with a thick wall of bone separating the foramina acusticum superius (lateral) and inferius (medial). Many small foramina for the passage of branches of the cochlear nerve are observed within the walls of the foramen acusticum inferius. Posterior to the internal auditory meatus is the anteriormost portion of the subarcuate fossa, but most of the structure is missing because of damage.

Two openings at the broken anterior edge of the subarcuate fossa expose the course of the vestibular apparatus of the inner ear. The medial of these openings exposes the anterior limb of the anterior semicircular canal (which surrounds the opening of the subarcuate fossa when it is complete), and the lateral opening exposes the crus commune.

The sulcus for the inferior petrosal sinus extends across the medial edge of the petrosal in an anterior-posterior direction. The petrosal contribution to this sulcus (which provides an intramural course for the inferior petrosal sinus) is not smooth, but rather pitted. The texture of the sulcus likely is the result of taphonomic wear after the petrosal was isolated from the rest of the skull. The canaliculus cochlearis opens near the posterior terminus of the sulcus for the inferior petrosal sinus, on the medial surface of the petrosal. The aperture of the cochlear canaliculus is small, circular, and opens into a short, posteriorly directed sulcus.

The promontorium contributes to most of the tympanic surface of the petrosal (Fig. 3C, D). The promontorium is inflated. The surface of the promontorium is abraded, but it lacks any major sulci. A shallow, elongate depression is at the anterolateral aspect of the promontorium. This depression likely contributes to the fossa for the tensor tympani muscle.

The fenestrae vestibuli and cochleae open along the lateral and medial aspect of the posterior edge of the promontorium respectively. A shelf for the footplate of the stapes circles the inside of the fenestra vestibuli, but the stapes itself is not preserved. In the absence of the stapes, dimensions of the fenestra vestibuli were used as a proxy for measuring the stapedial ratio (see Segall 1970). The stapedial ratio for URBAC 03-150 is 1.57, indicating a round fenestra vestibuli. The oval fenestra cochlea is smaller than the fenestra vestibuli. The crista interfenestralis, which is the bridge of bone separating the two fenestrae, is broad. This is a result of the diminutive size of the fenestra cochleae.

Posterior to the promontorium is an additional opening where the petrosal is broken. The damaged area exposes the posterior semicircular canal near the junction of the posterior ampulla and posterior semicircular canal.

The primary facial foramen is anterolateral to the fenestra vestibuli. The foramen is circular, and no bone floors the ventral side of the canal. As a consequence, there is no separation between the primary facial foramen and the hiatus Fallopii. Matrix fills the facial canal, so a connection through to the internal auditory meatus cannot be observed.

The sulcus for the facial nerve extends posteriorly from the primary facial foramen before curving medially. A small notch followed by a short, horizontal groove is immediately posterior to the sulcus of the facial nerve, opposite the primary facial foramen. The petrosal is damaged in this area, but the location of this groove implies that it is the dorsal portion of the prootic canal. The prootic canal is situated in the same manner in *Deltatheridium* (Rougier *et al*. 1998, fig. 3). If the petrosal were complete, the canal would be developed as an enclosed tube within the petrosal.

Upper dentition

The upper incisors are not known.

A single, isolated, upper canine CCMGE 5/11758 is referable to *Sulestes* (Nessov 1981, fig. 9(22), 1982, pl. 1, fig. 8; Nessov & Kielan-Jaworowska 1991, fig. 1). The canine is large, over 12 mm in total height, with the distal edge almost straight and the mesial edge strongly convex. The tooth is labiolingually compressed, with a maximum W/L ratio of 60%. The crown-root boundary is hardly detectable and is marked by a slight constriction. The crown is relatively low, occupying only 20% of the tooth height. The crown apex is deflected distally. A prominent wear facet is incised into the labial side at the coronal apex. The root gradually tapers towards the basal end. Both sides of the root are covered by faint longitudinal ridges. These ridges are more pronounced on the labial side. On this side as well a narrow longitudinal groove extends for most of the length of the root. CCMGE 5/11758 is referred to *Sulestes* because it fits the canine alveolus in CCMGE 42/12000 and bears longitudinal ridges possibly corresponding to the grooves in that alveolus (see above). A similar upper canine with low crown and long root can be seen in some specimens of Mongolian *Deltatheridium* (AMNH 21706; Gregory & Simpson 1926, figs 6, 7). An alternative, less likely interpretation of CCMGE 5/11758 is that it could belong to a large zhelestid from Dzharakuduk, some of which also have enlarged, single-rooted canines.

The upper permanent premolars are not known (except for the coronal apex of P3 erupting in URBAC 04-164; Fig. 2A, B). Judged from their alveoli, P3 was the largest and P1 was the smallest upper premolar. All upper permanent premolars were double-rooted.

The DP3 is known from a single specimen in situ (URBAC 04-164; Fig. 2A, B). In occlusal view, its crown is in the form of an isosceles triangle pointed distolabially. The paracone and metacone are of roughly equal size and height; both are very low. The metacone is positioned more lingually than the paracone. The postmetacrista is a prominent shearing blade set at a right angle to the centrocrista. The stylar shelf is wide at the metacone but drastically decreases in width mesially and is totally lacking labial to the paracone. The labial side of the tooth is straight, without an ectoflexus. The labial cingulum occupies the labial margin except in the area labial to the paracone. The labial cingulum is worn and its widening distal to the paracone suggests that at least one cingular cusp (cusp C) may have been present on the ectocingulum. The parastyle is well developed; a paracingulum connects with the parastyle. A short, narrow parastylar groove is mesial to the paracingulum. No metacingulum is present. The trigon is very small and is triangular, with a hardly discernable protocone and a shallow trigon basin. No conules are developed (a paraconule might have been present, but was eliminated by wear). The tooth possibly has three roots.

The upper molars are known from three dentigerous maxillary fragments (URBAC 04-164 with M1 [Fig. 2A, B], CCMGE 35/1200 with M1-2 [holotype, not figured here], and URBAC 04-149 with M2-3 [Fig. 2C, D]) and two isolated teeth (URBAC 04-345, M1 [Fig. 2E-H] and URBAC 99-017, M2 [Fig. 2I-L]). Only M4 is unknown. Isolated upper molars of *Sulestes* can be readily identified because most of the molars are known in situ and teeth at the four positions are markedly different morphologically from each other. All upper molars have three roughly equal roots (see above description of alveoli).

The M1 and M2, with symmetrical crowns, are more similar to each other than either is to the asymmetrical M3. The crown of M1 is of triangular outline, with a deep ectoflexus. The deepest point of the ectoflexus is at the level between the bases of the paracone and the metacone. The mesial side of the crown is noticeably shorter than its distal side. The paracone and the metacone are located at the buccolingual center of the crown, separating an extensive stylar shelf and a relatively small trigon. The paracone is a little taller than the metacone. The metacone is more labiolingually compressed than the paracone. The cusps are connected by a straight and high centrocrista, elevated well above the level of the trigon basin and stylar shelf. The preparacrista is directed almost labially, short and concave in mesiodistal view, connecting the stylocone (CCMGE 35/12000) or parastyle (URBAC 04-164). The stylocone is large, ridge-like, and labiolingually compressed. The parastylar wing is poorly developed. The parastyle is a distinct cusp, much smaller than the stylocone and attached to the base of the latter. The postmetacrista is long, straight, blade-like and directed distolabially. A weakly differentiated postmetacrista cusp (cusp 'c' of Crompton 1971) is present in CCMGE 35/12000 but absent on two other specimens. The stylar shelf reaches its greatest width labial to the metacone. The ectocingulum is well developed, with five minute cingular crenulations, increasing in size distally (CCMGE 35/12000), or with a single cingular crenulation in the position of the stylar cuspule C, opposite the notch between the paracone and the metacone (URBAC 04-164 and 04-345; Fig. 2F). The trigon is small, about 30% of the posterior crown width, and tapers lingually. The protocone is low, approximately half the height of either the paracone or metacone, and ridge-like, with a concave labial wall and a convex lingual wall. The paraconule and the metaconule are minute cusps approximating the base of the protocone, with poorly differentiated to absent internal cristae (in URBAC 04-164 the metaconule is absent or obliterated by wear). The paracingulum (preprotocrista) is rather long, extending mesiolabially toward the parastyle. In CCMGE 35/12000 there are two minute crenulations on the preprotocrista just labial to the paraconule (absent on two other specimens). A narrow parastylar groove dissects the paracingulum distal to the parastyle in a worn specimen (URBAC 04-164). The postprotocrista is much shorter, terminating at the base of the metacone; hence, the metacingulum is absent.

Table 1. Upper molars measurements (in mm) of *Sulestes karakshi*, Dzharakuduk, Uzbekistan; Late Cretaceous (Turonian).

Tooth/Specimen	Measurements		
	L	AW	PW
M1			
URBAC 04-164	2.1	2.1	2.3
CCMGE 35/12000	2.2	2.2	2.3
URBAC 04-345	—	—	2.5
M2			
URBAC 99-017	2.3	2.5	2.5
URBAC 04-149	2.3	2.7	2.7
CCMGE 35/12000	2.5	2.8	2.9
M3			
URBAC 04-149	2.1	2.9	2.0

The M2 is about 12% larger than M1 (Table 1). The main difference between the two adjacent molars is that in M2 the parastylar region is better developed and the length differential between mesial and distal sides of the crown triangles is less than in M1; consequently, the crown of M2 is more symmetrical than that of M1. The preparacrista contacts the stylocone in all specimens. The stylocone is a large cusp (taller than in M1) in CCMGE 35/12000 and URBAC 99-017, with a triangular base in the latter specimen, but distinctly smaller in URBAC 04-149 (Fig. 2C, D, J, L). On the ectocingulum a minute crenulation is developed distal to the stylocone (URBAC 99-017 and 04-149), or two small crenulations distal to the ectoflexus notch (CCMGE 35/12000). The M2 trigon and protocone seem proportionally larger than in M1. The conular internal cristae are slightly better developed compared with M1.

The M3 is known from a single specimen in situ (URBAC 04-149; Fig. 2C, D). In contrast with M1-2, the crown of M3 is asymmetrical, with a hypertrophied parastylar wing and a strongly reduced metastylar wing. The metacone is also reduced, being approximately half the volume and height of the paracone, and the metaconule is indistinct, although an extremely faint premetaconule crista is present. The paraconule is similar in size to that cusp in M2, with a similarly developed postparaconule crista. The postmetacrista is short, low, and distally convex. The ectoflexus is shallow and the ectoflexus notch is much closer to the distal

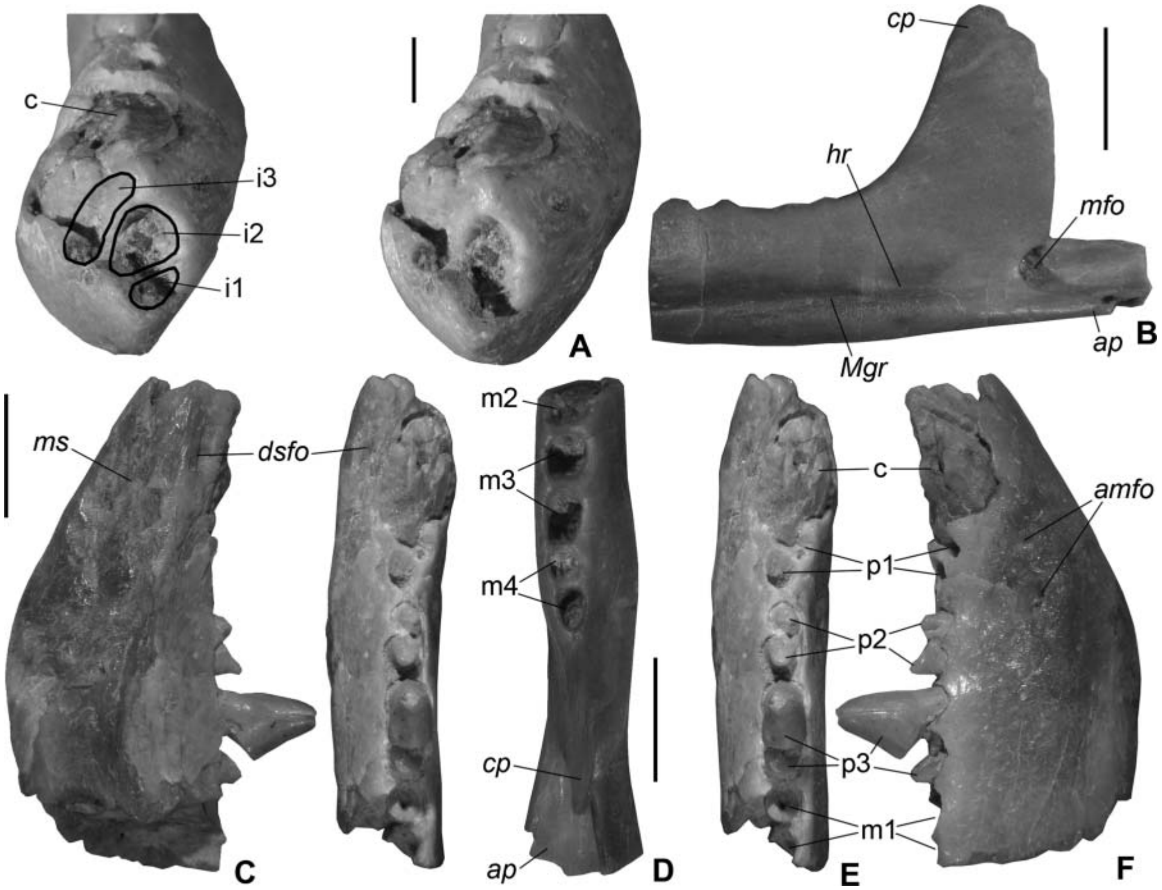

Figure 4. Dentary fragments of *Sulestes karakshi* Nessov, 1985 from the Turonian Bissekty Formation of Dzharakuduk, central Kyzylkum Desert, Uzbekistan. **A, C, E, F,** URBAC 00-057, fragment of a right dentary with broken c, p3, alveoli for i1-3, p1, m1, and roots of p2, in mesial (**A**, stereopair), lingual (**C**), occlusal (**E**, stereopair), and labial (**F**), views; **B, D,** URBAC 06-006, fragment of a right dentary with alveoli for m2-4 and partially preserved coronoid and angular processes, in lingual (**B**) and occlusal (**D**) views. Scale bar equals 1 mm (**A**) and 3 mm (**B-F**). Abbreviations: amfo, anterior mental foramen; cp, coronoid process; dsfo, dorsal symphyseal foramen; hr, horizontal ridge; mfo, mandibular foramen; Mgr, Meckelian groove; ms, mandibular symphysis.

margin of the crown than in M1-2. No crenulations are developed on the ectocingulum. The preparacrista is transverse near the paracone, but its labial portion is mesially deflected towards the stylocone, which is quite small and occupies a more mesial position compared with M1-2. The parastyle is even smaller and attached to the base of the stylocone. The parastylar groove intersects the preparacrista distal to the stylocone in contrast with M1-2, in which this groove is always mesial to the preparacrista and the stylocone. The protocone is of about the same size as in M2.

As can be deduced from M4 alveoli preserved in URBAC 04-149 and ZIN 90312 (Fig. 2C), M4 was an asymmetrical tooth like M3, possibly a 20% reduced copy of that tooth. An unreduced talonid on m4 suggests that the protocone on M4 was unreduced and set in line with the protocone of other upper molars, as is also indicated by the lingual alveolus for M4.

Dentary

Although no complete dentary of *Sulestes* has been discovered, a number of different fragments cover the dentary morphology fairly well (Figs 4, 5). In lateral view the horizontal ramus of the dentary is relatively deep, exceeding about twice the height of the molars (deepest between m3 and m4). The ventral border is arched ventrally while the alveolar border is nearly horizontal. The depth of the horizontal ramus is somewhat increased at the posterior end of the mandibular symphysis but more anteriorly it decreases markedly in depth, with the ventral border slanting toward the alveolar border at an angle of about 35° (Figs 4C, F, 5K-M). The horizontal ramus is very thin at the alveoli for the incisors. The incisor alveolar border is somewhat elevated dorsally relative to the postcanine alveolar border. The horizontal ramus markedly increases in depth ontogenetically. Posteriorly, the largest (ZIN 82620) and smallest (URBAC 03-104) specimens differ by 1.8 times in the depth

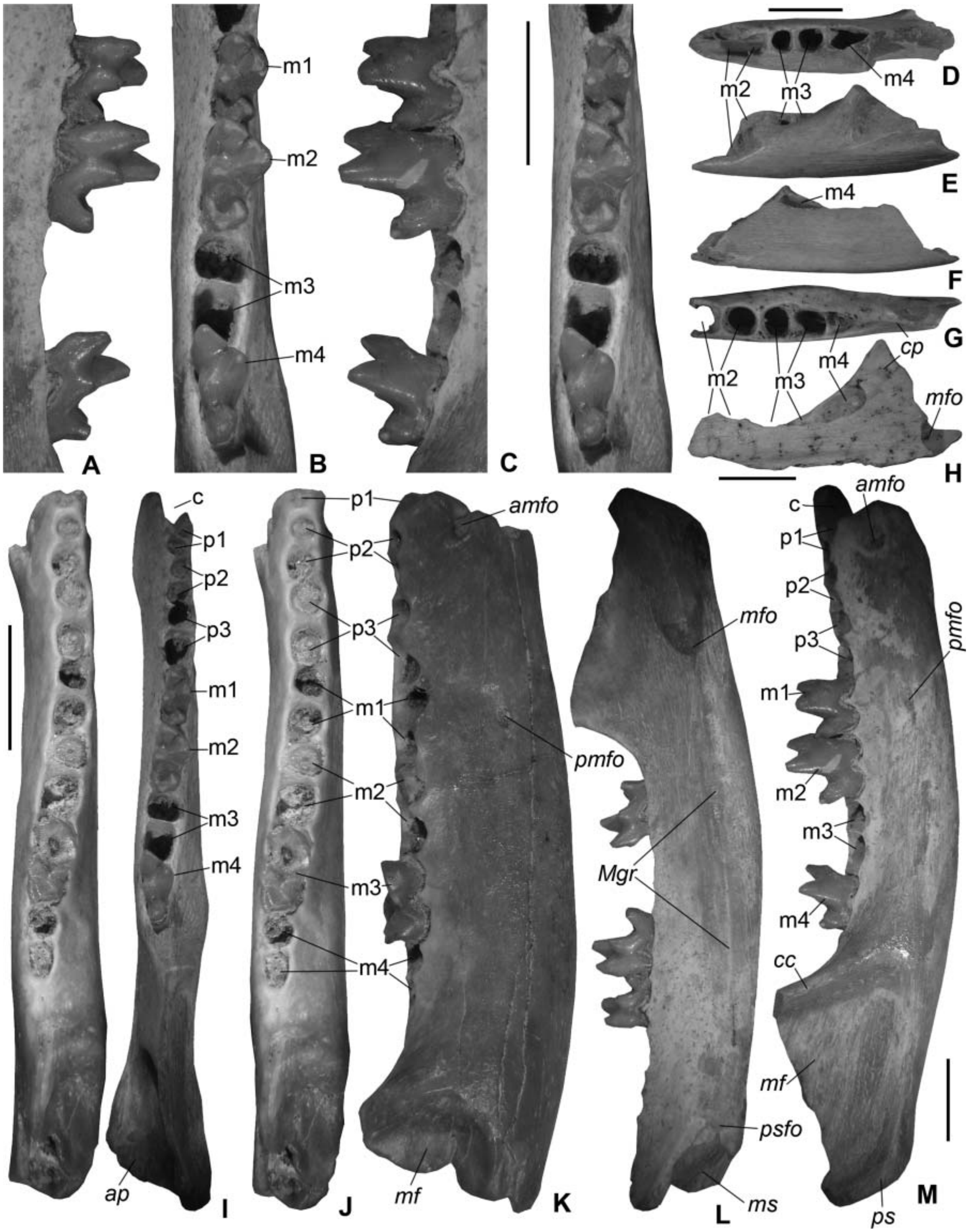

Figure 5. Dentary fragments of *Sulestes karakshi* Nessov, 1985 from the Turonian Bissekty Formation of Dzharakuduk, central Kyzylkum Desert, Uzbekistan. **A-C, I, L, M,** URBAC 06-005, almost complete right dentary with m1, 2, 4 and alveoli for c, p1-3, and m3, in lingual (**A**, **L**), occlusal (**B**, stereopair, **I**), and labial (**C**, **M**) views; **D-F,** URBAC 03-104, fragment of a left juvenile dentary with alveoli for m2-4, in occlusal (**D**), labial (**E**), and lingual (**F**) views; **G, H,** CCMGE 16/11758, fragment of a right juvenile dentary with alveoli for m2-4, in occlusal (**G**) and lingual (**H**) views; **J, K,** ZIN 89007, fragment of a right dentary with m3 missing most of the crown and alveoli for p1-3, m1, 2, 4, in occlusal (**J**, stereopair) and labial (**K**) views. Scale bar equals 3 mm. Abbreviations: amfo, anterior mental foramen; ap, angular process; cc, coronoid crest; cp, coronoid process; mf, masseteric fossa; mfo, mandibular foramen; Mgr, Meckelian groove; ms, mandibular symphysis; pmfo, posterior mental foramen; ps, posterior shelf; psfo, posterior symphyseal foramen.

of horizontal ramus at the ascending ramus. Anteriorly the largest (URBAC 00-057) and smallest (ZIN 88486) specimens differ by 1.9 times in the depth of the horizontal ramus at the posterior end of the mandibular symphysis.

The alveolar margin contains alveoli for three incisors, canine, three premolars, and four molars. No distinct diastemata are developed between the teeth and interradicular spaces are larger than the inter-dental spaces. The latter may be absent altogether in juvenile specimens, with the alveoli for adjacent teeth confluent. The alveolar border is higher medially than laterally, so the alveoli are visible in lateral, but not in medial view (except the alveolus for the erupting m4, see below).

The incisor alveoli are present only in one specimen (URBAC 00-057; Fig. 4A). They are posteroventrally oblique, parallel to the ventral border of the dentary. The alveolus for i2 is the largest and the alveolus for i3 is the smallest. The i2 alveolus is evidently staggered between the alveoli for i1 and i3; its ventral border is placed dorsal to the ventral borders of the other alveoli (Fig. 4A). Although not complete, the mesial bony buttress for i2 apparently projected anterodorsally above the alveolar borders for i1 and i3. A small, possibly vascular, foramen opens on the alveolar bony buttress for i2.

A single, very large alveolus held the lower canine (Figs 4A, 4E, 5C). It is slanted posteroventrally, but somewhat more vertical, than the alveoli for the incisors. The distal end of the canine alveolus is at the posterior end of the mandibular symphysis. The long axis of the canine alveolus is more or less parallel to the symphyseal margin and inclined at an angle ~25° to the axis of postcanine teeth.

Six alveoli are double rooted for p1-3. The alveoli for p3 are the largest and the alveoli for p1 are the smallest (Figs 4E, 5I, J). The p1 anterior root alveolus is distinctly smaller than the posterior root alveolus, whereas in p2 and p3 the anterior root alveolus is only marginally smaller than the posterior root alveolus. The alveoli for p1 in most cases (except URBAC 03-184) are placed oblique to the postcanine alveolar axis, but parallel to the canine alveolus. Normally the alveoli for p2 are in line with other postcanine alveoli, but could be also obliquely set (ZIN 88467 and 88486), although not so oblique as the alveoli for p1. The alveoli for p3 are similar to or larger in size than the alveoli for m1.

Eight alveoli are for double rooted m1-4 (Figs 5I, J). The largest are the alveoli for m3, the smallest are the alveoli for m4, which, however, are only slightly smaller than the alveoli for m1. In all molars the alveolus for the posterior root is somewhat longer (anteroposteriorly) than the alveolus for the anterior root (this length differential is most evident for m4). In juvenile specimens (CCMGE 16/11758, URBAC 02-023 and 03-104; Fig. 5D-H) the alveoli for the erupting m4 are on the ascending ramus of the dentary, above the alveolar borders of other postcanine teeth. This alveolus is seen from the medial, but not from the lateral side. At this ontogenetic stage, the alveoli for the m4 roots are confluent. In a somewhat later stage (ZIN 90309, URBAC 03-090, 03-222) the interradicular bony septum of m4 is present but incomplete. In adult specimens this septum is complete and m4 is on the horizontal ramus, separated some distance from the ascending ramus.

The anterior mental foramen is usually large and placed between p1 and p2 (Figs 4F, 5K, M). Sometimes it is smaller and is at the level of the anterior root of p2 (ZIN 82620 and 89008). A double anterior mental foramen is present in URBAC 00-057 (between c and p1 and between p1 and p2; Fig. 4F) and URBAC 03-184 (at the level of p1 and between p1 and p2). The posterior mental foramen is normally smaller than the anterior mental foramen and placed in most specimens under m1 (Fig. 5K, M; between m1 and m2 in ZIN 88467 and URBAC 03-043). In ZIN 90310 it is slit-like and much larger, being nearly equal to m1 in length.

Anteriorly, there is a marked medial projection of the horizontal ramus is present at the symphysis. The mandibular symphysis is an oval-shaped, roughened area that starts at the anterior end of the dentary and extends posteriorly to the level of p2 (most specimens), between p2 and p3 (URBAC 03-043), or the level of p3 (URBAC 00-057; Fig. 4C). As the mandibular symphysis is most posteriorly extended in the largest specimen in the sample (URBAC 00-057), the posterior expansion of the mandibular symphysis appears to be an ontogenetic trait. The long axis of the mandibular symphysis is inclined at an angle of approximately 30° to the alveolar border. The posterior symphyseal foramen can be recognized in the majority of specimens (Fig. 5L), except in the largest specimen, URBAC 00-057. This foramen is a rather small circular or slit-like opening at the posterior border of the mandibular symphysis, approximately at the level of the Meckelian groove. The depression is blind except for one or several tiny openings into the mandibular canal. In smaller specimens (e.g. ZIN 88486) the dorsal border of the mandibular symphysis closely approximates the alveolar border, while in the largest specimen (URBAC 00-057) a larger space separates them (Fig. 4C, E). In the latter specimen, a distinct dorsal symphyseal foramen opens between the mandibular symphysis and the canine (Fig. 4C, E).

A Meckelian groove, which varies greatly in extent and distinctness (e.g. Fig. 4B), is present in 11 of 16 relevant specimens (69%). The best developed Meckelian groove is in URBAC 06-005 (Fig. 5L), where it is relatively shallow, straight and extends between the mandibular foramen and the level of p3. Anteriorly this groove is parallel with the inferior border of the dentary. In other specimens it is shorter anteriorly and/or vanishes posteriorly before reaching the mandibular foramen. A short, weak horizontal ridge just above the posterior end of the Meckelian groove, possible delimiting the ventral extent of the temporalis muscle attachment (Wible 2003; Fig. 4B), can be seen in URBAC 06-006 and 02-023.

The horizontal ramus gradually continues into the ascending ramus without constriction. The coronoid process was completely preserved only in ZIN 88130 but is now dorsally broken. The undamaged condition can be seen in Nessov (1985b, pl. 2, fig. 5b, 1997, pl. 47, fig. 1v) and Averianov (2000, fig. 28.5L). The anterodorsal tip of the coronoid process is preserved also in URBAC 06-006 (Fig. 4B). The ascending ramus is almost three times higher than the horizontal ramus, with a rather steep anterior border of the coronoid process, sloping at an angle of 70–72° toward the alveolar margin. The masseteric fossa is very large and deep, extending posteriorly to the condylar process, and bordered anteriorly by a very prominent, sharp, and high coronoid crest (Fig. 5M). Ventrally the masseteric fossa is bordered by an extensive posterior shelf (Fig. 5M). The larger anterior portion of the posterior shelf is horizontal and widens posteriorly. A shorter posterior portion of the shelf is directed posteroventrally and buttresses the mandibular condyle. The posterior border of the coronoid process is thin and concave. Within the masseteric fossa at the ventral end of the coronoid crest normally there are several irregular vascular foramina but a true labial mandibular foramen is lacking.

The condylar process is preserved only in ZIN 88130 (Nessov 1985a, pl. 2, fig. 5, 1997, pl. 47, fig. 1; Averianov & Kielan-Jaworowska 1999, fig. 2). The mandibular condyle is distinctly above the alveolar level. The condyle is convex, oval in posterior view, with the medial side wider and placed more dorsally compared with the pointed lateral end. The articular surface of the condyle is not completely preserved.

The angular process is not posteriorly complete on any specimen (Figs 4B, 4D, 5I). Its proximal portion is a thin shelf along the medioventral margin of the ascending ramus, oriented at approximately 90° to the plane of the coronoid process, i. e. completely medially inflected. The angular shelf widens considerably posteriorly and its posterior border was apparently concave. The angular process in *Sulestes* possibly matches the rod-like or intermediate category of the marsupial angular processes (Sánchez-Villagra & Smith 1997), although the rod itself is not preserved.

The medial side of the coronoid process is vertical and remarkably flat. The mandibular foramen is relatively large, circular, and posteriorly directed. It opens immediately above the angular process in the middle of the ascending ramus (Figs 4B, 5L).

Lower dentition

The lower incisors are not known. Judging from their alveoli (see above), there were probably three lower incisors, i2 the largest and i3 the smallest.

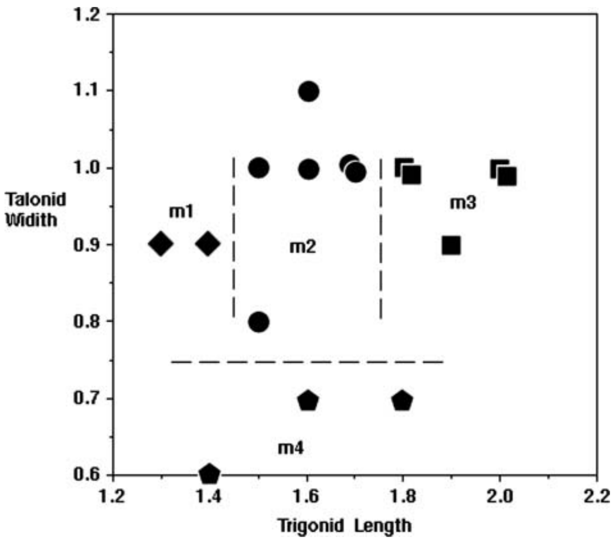

Figure 6. Bivariate plot (talonid width versus trigonid length) for lower molars of *Sulestes karakshi* Nessov, 1985.

The lower canine crown is not known and the canine root is preserved only in URBAC 00057 (Figs 4A, E, F). It is the longest (mesiodistally) tooth in the lower dentition. The root is single, not subdivided.

Among lower premolars, the crown is known only for p3, represented by a single specimen in situ (URBAC 00-057; Fig. 4C, E, F). The crown is high and cone-like, labiolingually compressed (the crown length exceeds twice the crown width). The mesial margin of the crown is almost vertical and is slightly convex, while the distal margin is more slanted and slightly concave. The unworn anterior crest is extremely faint. The posterior crest is more robust and worn. There are no anterior accessory cusp, nor cingulid. The posterior portion of the crown is missing and it is unclear if a posterior accessory cusp was present.

The collection includes a number of isolated lower molars and two dentaries bearing molars: URBAC 06-005 with complete m1, m2, and m4 (Fig. 5A-C, I, L, M), and ZIN 89007, with m3 missing the trigonid (Fig. 5J, K). This serendipitous distribution of lower molars preserved in dentaries, coupled with the noticeable differences between lower molar loci, allows quite precise identification of isolated lower molars. With the help of the associated lower molars, differences in lower molars are most obvious in a bivariate plot of talonid width versus trigonid length (Fig. 6). The talonid width is 0.8 mm or greater for m1-3, but 0.7 mm or less for m4. The m4 shows variation in trigonid length, while the m1-3 show a progressive increase in trigonid length (m1 equal or less than 1.4 mm, m2 between 1.5 and 1.7 mm, and m3 1.8 mm or longer).

In all lower molars the crown is higher labially than lingually and the distal root is somewhat longer (mesiodistally) than the mesial root.

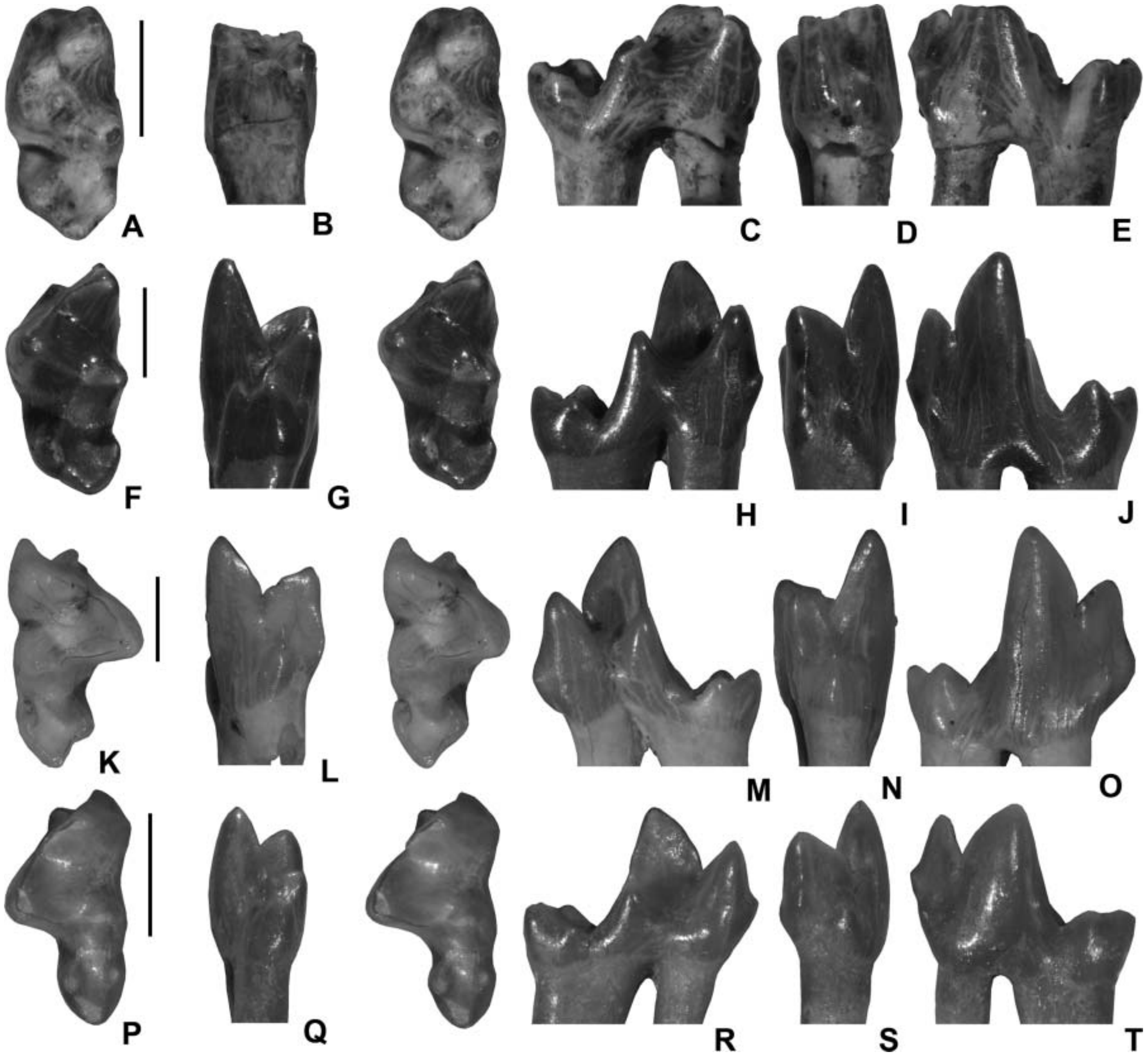

Figure 7. Isolated lower molars of *Sulestes karakshi* Nessov, 1985 from the Turonian Bissekty Formation of Dzharakuduk, central Kyzylkum Desert, Uzbekistan. **A-E,** URBAC 02-111, left m1, in occlusal **(A**, stereopair**)**, distal **(B)**, lingual **(C)**, mesial **(D)**, and labial **(E)** views; **F-J,** URBAC 03194, left m2, in occlusal **(F**, stereopair**)**, distal **(G)**, lingual **(H)**, mesial **(I)** and labial **(J)** views; **K-O,** URBAC 04-169, right m3, in occlusal **(K**, stereopair**)**, mesial **(L)**, lingual **(M)**, distal **(N)**, and labial **(O)** views; **P-T,** URBAC 04-346, left m4, in occlusal (**P**, stereopair), distal **(Q)**, lingual **(R)**, mesial **(S)**, and labial **(T)** views. Scale bar equals 1 mm.

The m1 is known from two specimens, in situ in URBAC 06-005 (Fig. 5A-C, I, L, M) and as an isolated specimen in URBAC 02-111 (Fig. 7A-E). The crown is dominated by a large trigonid; the talonid is distinctly shorter (22–35% of the tooth length; Table 2), but close to the trigonid in width (82% from the trigonid width; Table 2). In the trigonid the protoconid is the largest and most massive cusp, somewhat triangular in cross-section with the lingual side flattened. The paraconid is also massive, being only slightly lower than the protoconid. The metaconid is the smallest trigonid cusp, both in terms of height and size of its base. All trigonid cusps are vertically directed. The paracristid and protocristid are set obliquely relative to the long axis of the dentary, with the paraconid and the metaconid placed, respectively, mesiolingual and distolingual to the protoconid. The paracristid is more pronounced than the protocristid, with a better-developed carnassial notch. The trigonid basin is a lingually sloping triangular area between the bases of the trigonid cusps. It is open lingually by a narrow cleft between the separated bases of the paraconid and the metaconid. The mesiolabial cuspule f is precingulid-like and located at the mesial base of the trigonid opposite the paracristid notch. It is separated by a vertical groove from the smaller mesiolingual cuspule e, which is fully developed in URBAC 02-111 (Fig. 7D), while in URBAC 06-005 it is merely the vertical crest along the mesiolingual edge of the paraconid, which extends towards the apex of the paraconid. The distal wall of the trigonid is not

Table 2. Lower molars measurements (in mm, except TRA) of *Sulestes karakshi*, Dzharakuduk, Uzbekistan; Late Cretaceous (Turonian).

	Measurements					
Tooth/Specimen	L	TRL	TRW	TAL	TAW	TRA
m1						
URBAC 06-005	1.8	1.4	1.1	0.4	0.9	75°
URBAC 02-111*	2.0	1.3	1.1	0.7	0.9	—
m2						
URBAC 03-009	2.3	1.5	1.4	0.8	0.8	54°
URBAC 04-344	2.3	1.6	1.3	0.7	1.0	56°
URBAC 06-005	2.4	1.5	1.5	0.9	1.0	67°
URBAC 00-001	2.5	1.8	1.5	0.7	1.1	47°
CCMGE 5/12455*	2.6	1.7	1.5	0.9	1.0	—
URBAC 04-291	—	1.7	1.5	—	—	62°
URBAC 03-194	2.6	1.7	1.7	0.9	1.0	58°
m3						
URBAC 02-093*	2.6	1.8	1.3	0.8	1.0	—
URBAC 98-012*	2.6	1.8	1.4	0.8	1.0	—
URBAC 04-169	2.7	1.9	1.5	0.8	0.9	50°
URBAC 06-019*	—	1.9	1.8	—	—	—
CCMGE 40/12455	2.7	2.0	1.6	0.7	1.0	—
CCMGE 41/12455*	2.8	2.0	1.5	0.8	1.0	45°
ZIN 89007	—	—	—	1.0	1.1	—
m4						
URBAC 04-346	1.9	1.4	1.0	0.5	0.6	60°
URBAC 06-005	2.3	1.6	1.1	0.7	0.7	—
URBAC 04-217	2.6	1.8	1.5	0.8	0.7	50°

Note: *worn tooth.

vertical but sloping mesially. The distal metacristid is a distinct sharp crest extending distolabially from the metaconid apex toward the base of the hypoconid, where it is becomes confluent with the hypocristid. The protocone groove (see below) and a crest along the distolingual edge of the metaconid are not developed on either m1 specimen. The talonid is three cusped; the entoconid is distinct in URBAC 02-111 but poorly individualized in URBAC 06-005 (Fig. 5B). The hypoconid is the largest and the entoconid is the smallest talonid cusp, although the size and height differential between the cusps is not great. The hypoconulid is equidistant from the hypoconid and entoconid. The talonid basin is small and shallow, sloping mesiolingually. It is closed lingually by a low entocristid. The hypoflexid is a deep, triangular indentation extending lingually up to the half of the talonid width towards the contact point between the distal metacristid and the hypocristid. The area of the hypoflexid is distinctly smaller than the talonid basin.

Compared to m1, m2 is distinctly taller, on average 1.3 times longer, and 1.35 times wider (mean L = 2.45 ± 0.06, TRW = 1.49 ± 0.05). In addition to the in situ m2 (URBAC 06-005; Fig. 5A-C, I, L, M), there are three well-preserved and little-worn isolated m2s (URBAC 00-001, 03-009, and 03194; the last specimen is the most nearly complete and is figured in Fig. 7F-J). There are a few consistent details that distinguish m2 from m1. The trigonid angle is smaller, 47–67°, M = 57.33° ± 2.80 compared with 75° in m1 in URBAC 06-005, the only m1 specimen where the trigonid angle can be measured. The protocristid is more transverse compared to m1. The mesial cingulid structures are more pronounced than in m1. The mesiolabial cuspule f is a prominent precingulid extending labially toward the base of the protoconid. The mesiolingual cuspule e is a knob-like projection on a very sharp vertical crest extending toward the apex of the paraconid. The height of the metaconid is variable: in some specimens (e.g. URBAC 00-001 and 03-194) it is relatively lower than in other specimens (e.g. URBAC 03-009 and 06-005). A well-developed subvertical crest is present along the distolingual edge of the metaconid, contacting the entocristid and bordering lingually a shallow valley, the protocone groove, which is bordered labially by the distal metacristid. The talonid cusps are better developed than in m1, but the entoconid can be totally lacking (URBAC 04-344). In URBAC 06-005 a small entoconid is situated close to the hypoconulid, while in CCMGE 5/12455 and URBAC 03-194 the entoconid is larger and the hypoconulid is equidistant from the hypoconid and the entoconid (Figs 5B, 7F).

The m3 is somewhat larger (mean L = 2.68 ± 0.04, TRW = 1.52 ± 0.07) than m2 but very similar in structure to the latter. The most nearly complete unworn isolated m3 is URBAC 04-169 (Fig. 7K-O). The trigonid angle is smaller than in m2, 45–50°, mean = 47.5° ± 2.50. It seems that the metaconid is more reduced, both in height and mesiodistal length, compared with m2. The entoconid can be very small (CCMGE 40/12455) or totally lacking (ZIN 89007).

The structure of m4, known from three specimens, in situ in URBAC 06-005 (Fig. 5A–C, I, L, M) and isolated in URBAC 04-217 and 04-346 (Fig. 7P-T), is quite variable. The m4 is smaller than m2-3 but larger than m1 (L = 2.27 ± 0.20, TRW = 1.20 ± 0.15). The trigonid angle is 50–60°, mean = 55.00° ± 5.00, which is close to that in m2. The height differential between the paraconid and the metaconid is the largest among lower molars. The paraconid is high and directed mesiodorsally (URBAC 06—005) or dorsally (two other specimens). The metaconid is very small. The protocristid is more oblique than in m2-3, but similar in orientation with that in m1. The precingulid (mesiolabial cuspule f) is shorter than in m2-3. The talonid is much narrower and relatively longer than in the other lower molars. The hypoconulid is distally projected. The talonid basin is relatively smaller than in other lower molars; in URBAC 06-005 it looks merely like the continuation of the protocone groove sloping from the distal wall of the talonid (here the talonid is distally incomplete). In this specimen the entocristid is not well developed and the entoconid may possibly be lacking. In two other specimens the entocristid is better developed, with a minute entoconid present in URBAC 04-346 (Fig. 7P). In URBAC 04-217 the entoconid has been worn away, if it was ever present. The mesiodistal length differential between the roots is greater in m4 compared with other lower molars.

Measurements

C: CCMGE 5/11758: L = 1.9; W = 1.2 (crown); L = 2.5; W = 1.5 (root). DP3: URBAC 04-164: L = 1.6; W = 1.2. p3: URBAC 00–057: L = 2.4; W = 1.2. For measurements of molars see Table 1 (upper molars) and Table 2 (lower molars).

Taxonomic history of metatherians from the Bissekty local fauna

Nessov (1985b) referred *Sulestes karakshi*, at that time known only from the holotype, to the monotypic Sulestinae within Deltatheridiidae. Nessov (1987) and Kielan-Jaworowska & Nessov (1990) attributed to *Sulestes* sp. a dentary fragment with a heavily worn lower molar and a tooth fragment in front of it, CCMGE 5/12455. They thought that it may belong to a distinct species because the specimen was found at a lower stratigraphic level. We have not found any differences between mammalian and other vertebrates assemblages from different levels within the Bissekty Formation and thus we recognize all vertebrates from this stratigraphic unit as the single Bissekty local fauna (Archibald & Averianov 2005). More importantly, taxonomic attribution should be based on morphologic, not stratigraphic grounds.

In 1993 Nessov described a new deltatheroidan from Dzharakuduk, *Deltatheroides kizylkumensis*, represented by two isolated lower molars (in Nessov *et al*. (1994, p. 65) this deltatheroidan is mentioned as belonging to a new genus). He (Nessov 1993, p. 122; Nessov *et al*. 1994, p. 65) distinguished this species from *Sulestes* sp. by its "much larger size", metaconid more strongly reduced, but other cusps "much higher and sharper." With larger sample sizes and unworn teeth, such presumed taxonomic differences are no longer valid.

In Nessov's posthumous monograph, published in 1997, *Deltatheroides kizylkumensis* was referred to a new genus, *Deltatherus*. Nessov (1997, p. 163) distinguished *Deltatherus* from *Sulestes* by "approximately one and a half—two times larger size, apparently slightly more posterior position of the infraorbital foramen, and somewhat higher and sharper cusps of lower molars." As noted above, these differences in size and height/sharpness of molar cusps are not justified based on our larger samples. In CCMGE 42/12455, referred by Nessov to *Deltatherus*, the infraorbital foramen is placed at the boundary between P2 and P3. The holotype of *S. karakshi* is broken anteriorly at the level of the anterior root of P3 and does not preserve the infraorbital foramen. Thus there are no grounds for assessing the difference in position of the infraorbital foramen between these two specimens to be of taxonomic validity.

In the same monograph, Nessov (1997, p. 164) described a new genus and species, *Marsasia aenigma*, provisionally referred to Marsupialia. The taxon was based on two edentulous dentary fragments (the holotype, ZIN 82620, a nearly complete dentary preserving much of the ascending ramus, and the paratype, ZIN 83130, a posterior dentary preserving much of the ascending ramus including the mandibular condyle). The allocation to Marsupialia was based on the postcanine dental formula p1-3, m1-4, inferred from the alveoli, and a medially inflected shelf-like angular process. Averianov & Kielan-Jaworowska (1999) concurred in referring these two specimens to Marsupialia and referred an additional dentary fragment with a last molar (ZIN 83131) to *Marsasia* sp. (the latter is now referred to *Paranyctoides*, Archibald & Averianov 2005.) Attribution of *Marsasia* to Deltatheroida was rejected by Averianov & Kielan-Jaworowska (1999, p. 78) based on the observation that in "deltatheroidans the posterior root of the molars is smaller than the anterior one, because of the small size of the talonids." This observation, however, is in error: in all lower molars of all known deltatheroidans, the posterior molar root is somewhat larger, or of the same size, as the anterior root (Fig. 7). Another source of confusion was an incorrect reconstruction of the dentary of *Deltatheridium* as gradually tapering toward the anterior end (Kielan-Jaworowska 1975, fig. 5), whereas in *Marsasia* the dentary is noticeable deepened at the symphysis. Discovery of better-preserved specimens of *Deltatheridium* (Rougier *et al*. 1998, fig. 2) showed that in this respect the dentary of *Deltatheridium* does not differ from that of *Marsasia*. Finally, the finding of two dentary fragments with the morphology of *Marsasia* but with dentitions of *Sulestes* (ZIN 89007 and URBAC 06–005) unconditionally showed synonymy of these two taxa. Thus it is not surprising that *Marsasia* and *Sulestes* appeared as successive taxa on the cladograms of Luo *et al*. (2003) and Luo & Wible (2005).

As with other mammalian taxa from the Bissekty local fauna, a meaningful taxonomic revision of deltatheroidans became possible only after obtaining a larger sample (currently there are 42 specimens of *Sulestes karakshi*). In addition to the earlier discussed ontogenetic deepening of the dentary, it should be noted that some of the size variation within the sample of molars possibly reflects sexual dimorphism. The number of known molars is insufficient to demonstrate this statistically. At the moment we consider the known metatherian sample from the Bissekty Formation as representing a single biological species, *Sulestes karakshi*. *Sulestes* is the second best known deltatheroidan after the Mongolian Campanian *Deltatheridium*.

Postcrania of mammals from the Late Cretaceous of Uzbeksitan have been treated elsewhere (Szalay & Sargis 2006; Chester *et al*. 2007). Szalay & Sargis (2006) recognized as many as five metatherians (referred to as marsupials by these authors) based on tarsals. Until further comparisons can be made of Late Cretaceous tarsal elements, we regard referral of some of these tarsals to Metatheria as premature with the possibility that some of them may belong to Zhelestidae (Archibald & Averianov 2007). Chester *et al*. (2007) have identified humeri indicating two arboreal methatherians at Dzharakuduk.

Phylogenetic analysis of *Sulestes* and basal tribosphenidan and metatherian taxa

Deltatheroidans were the subject of several preliminary cladistic analyses (e.g. Cifelli 1993a, b; Averianov & Skutschas 1999), but the first comprehensive analysis of basal metatherians and related taxa was made by Rougier *et al*. (1998; see also Wible *et al*. 2001) in connection with discovery of new, better preserved specimens of *Deltatheridium* from Mongolia. Later, Rougier *et al*. (2004) published an updated version of this analysis incorporating new data. For our analysis we used a modified version of the data matrix of Rougier *et al*. (2004; Appendicies 1 and 4). We removed from the matrix taxa known only from one or two isolated teeth (*Aegialodon*, *Comanchea*, *Zygiocuspis*, *Falepetrus* and the North American Late Cretaceous unnamed deltatheroidans), and added three taxa (*Amphitherium*, *Montanalestes* and *Oklatheridium*). We removed also suprageneric terminal taxa (dryolestoids, Borhyaenidae and dasyurids) and Recent marsupial genera (*Marmosa*, *Didelphis*, and *Dromiciops*), leaving in the matrix only Mesozoic and Paleocene genera. The matrix was further modified by removing phylogenetically uninformative characters found by the Winclada version 1.00.08 program (Nixon 1999) and recoding of some characters states. The list of characters employed in the phylogenetic analysis is in Appendix 1, and the taxon-character matrix in Appendix 2. Below we provide comments for selected taxa and describe an evolutionary scenario of therian dental evolution near the metatherian-eutherian dichotomy.

Comments on taxa

Mozomus. *Mozomus shikamai* Li *et al*., 2005 is based on a single dentary fragment with seven teeth from the Shahai Formation (Aptian-Albian) of the Badaohao coal mine in Liaoning, China (Li *et al*. 2005). It was described as a zatherian similar to *Kielantherium*. The talonids, however, are poorly preserved and in particular we see no basis for reconstructing the talonid with two cusps. Judging from the small size of the talonids, it is more likely a stem zatherian mammal. The preserved dentition of *M. shikamai* was interpreted originally as p3-5(?), m1-4, with p5(?) being submolariform. Comparison with stem zatherian taxa, such as *Nanolestes* and *Arguimus* (see Lopatin & Averianov 2006a), suggests that the submolariform tooth of *M. shikamai* with a widely open trigonid basin is likely the "partially molariform" m1 and thus the postcanine dental formula for this taxon should be p1-5, m1-5, as in *Nanolestes* and in contrast with *Arguimus*, which has four molars. *Mozomus* is not included in our phylogenetic analysis because it is not related to *Kielantherium*.

Kielantherium. This is a basal tribosphenidan (aegialodontid) from the Aptian-Albian Hövöör locality in the Gobi Desert, Mongolia, known previously from an isolated lower molar and dentary fragments with m1-4 and alveoli for four double-rooted, more anterior teeth. Lopatin & Averianov (2006b, 2007) recently reported another lower molar and a previously unknown upper molar of *Kielantherium gobiense* Dashzeveg, 1975 from Hövöör, which allows us to code some upper dentition characters for this taxon.

Atokatheridium. The genus is known from isolated upper and lower molariform teeth from the Early Cretaceous (Aptian or Albian) Antlers Formation in Oklahoma, USA (Kielan-Jaworowska & Cifelli 2001; Davis *et al*. 2008). The taxon was referred to ?Deltatheroida (Kielan-Jaworowska & Cifelli 2001) or Deltatheridiidae (Davis *et al*. 2008). The latter referral was heavily influenced by interpretation of a relatively large incomplete upper molar OMNH 63725 (Davis *et al*. 2008, fig. 1.5C) as M3 of *Atokatheridium*. This molar, however, differs from other upper molars of *Atokatheridium* by its larger size and distinctly wider stylar shelf, the same characters that make it similar to teeth of deltatheroidan *Oklatheridium* from the same fauna (Davis *et al*. 2008). We refer here OMNH 63725 to *Oklatheridium*. Our analysis does not confirm attribution of *Atokatheridium* to Deltatheroida, but rather as a basal tribosphenidan.

Potamotelses. This is a basal tribosphenidan mammal from the early Campanian (possibly late Santonian, see Eaton 2006) Milk River Formation at Verdigris Coulee, Alberta, Canada (Fox 1972). *Potamotelses* is known by isolated upper and referred lower molars. Isolated lower molars of *Potamotelses* sp. have been reported also from the Santonian Straight Cliffs Formation of Utah, USA (Eaton 2006). The number of molars is considered here as unknown for *Potamotelses* instead of counting four molars as done by Fox (1975). Rougier *et al*. (1998, 2004) followed Fox's (1975) interpretation of *Potamotelses* as having a preprotocrista that does not extend labially past the base of the paracone. A continuous, but heavily worn preprotocrista can be seen in a stereophotograph of the holotype of *P. aquilensis* Fox, 1972 (Fox 1972, fig. 1a), which does not differ from similarly worn specimens of *Sulestes*. *Sulestes* and *Potamotelses* apparently both possessed a double-rank prevallum/postvallid shear, a fundamental attribute of the tribosphenic dentition.

***Picopsis*.** This taxon is based on an isolated upper molar and a trigonid of a lower molar from the Milk River Formation at Verdigris Coulee, Alberta, Canada (see comment in the previous paragraph about age of this stratigraphic unit), and was referred originally to Theria *incertae sedis* (Fox 1980). Additional isolated molars of similar design have been reported from the same locality (Fox 1980, 1982), and from various Albian-Cenomanian, Cenomanian, Turonian and Santonian localities in Utah and Montana, USA (Eaton 1993, 2006; Kielan-Jaworowska *et al*. 2004; Davis & Davies 2005).

Kielan-Jaworowska *et al*. (2004, p. 422) remarked that upper molars of *Picopsis* resemble the deciduous premolars of Marsupialia. Indeed, DP3 of *Sulestes* (Fig. 2A), if found isolated, could be referred to "*Picopsis*" based on the diagnosis provided for this taxon. The lower molars referred to this or a similar taxon, with a widely open trigonid and a small paraconid, are also likely milk teeth. We cannot determine whether *Picopsis* is a valid taxon, but it may well be based on metatherian deciduous dental remains and is accordingly excluded from the phylogenetic analysis.

***Montanalestes*.** This is a tribosphenidan mammal named on a single, well-preserved dentary fragment with three molars, three posterior premolars, condylar, angular, and most of the coronoid processes from an unspecified locality within the Aptian-Albian Cloverly Formation of Montana, USA (Cifelli 1999). In the original description it was formally referred to Tribosphenida *incertae sedis*, but it was noted that it bears two "characteristics (molarized last premolar, reduction to three molars) otherwise known only for Eutheria among tribosphenic mammals" (Cifelli 1999, p. 363). Not surprisingly, in subsequent cladistic analyses, *Montanalestes* is invariably placed within the Eutheria (e.g. Luo *et al*. 2002, 2003, 2007a; Ji *et al*. 2002, 2006; Luo & Wible 2005; Li & Luo 2006; Meng *et al*. 2006; Wible *et al*. 2007).

We argue that the dental formula of five premolars and three molars, as interpreted for *Peramus* (see McKenna 1975), is basal for Theria (see the next section), rather than being a "reduction to three molars" (Cifelli 1999, p. 363) in the eutherian lineage. Thus, although the presence of three molars is the case for the vast majority of eutherians, it is most likely a plesiomorphic retention from a common therian ancestor.

The small cusp at the very base of the distal margin of the ultimate premolar in *Montanalestes* may be homologous to a metaconid, but we do not agree that this characterizes the tooth as molariform (well-developed talonid and trigonid with three distinct cusps) or even semimolariform (moderately well-developed talonid and trigonid without all three distinct cusps). More importantly, its structure is close to that of the p5 of *Peramus*, which has the same distal accessory cusp and the same uniquely lingually placed mesial accessory cusp ("paraconid"). It seems most likely that the morphology of this tooth in *Montanalestes* is inherited from a *Peramus*-like ancestor rather than reflecting the distinctive eutherian morphology of a semimolariform p5 with a lingually placed metaconid and an incipiently basined talonid that first appears in the fossil record in the Cenomanian (*Bobolestes*).

Montanalestes also possesses three characteristics that are more normally associated with metatherians than with eutherians. These are: the paraconids of lower molars are similar in size and height or slightly taller than metaconids; on the mesiolingual edge of the paraconid a distinct cristid runs from the tip to near the base of the cusp; and the mandibular angle is lingually inflected although it does not form a well delineated shelf as is known in unquestionable Cretaceous metatherians. *Montanalestes* was considered a Cretaceous eutherian although it comes closest to the metatherian form of the mandibular angle (Wible *et al*. 2004, p. 37).

***Kokopellia*.** This is a basal metatherian known by several jaw fragments and isolated teeth from the Albian-Cenomanian Cedar Mountain Formation of Utah, USA (Cifelli 1993a; Cifelli & Muizon 1997). *Kokopellia* was coded by Rougier *et al*. (2004) as having no Meckelian groove, but a "faint trace" of this groove is present, as in the Paleocene metatherians from South America (Cifelli & Muizon 1997, p. 244; Kielan-Jaworowska *et al*. 2004, p. 433).

***Deltatheridium* and *Deltatheroides*.** New materials of these taxa from the Campanian of the Gobi Desert, Mongolia were the basis for a phylogenetic analysis by Rougier *et al*. (1998, 2004). At least one of their scorings for these taxa requires comment. Rougier *et al*. (1998, 2004) coded *Sulestes* as having stylar cusp A [parastyle] distinct, but smaller than B [stylocone], while *Deltatheridium* and *Deltatheroides* as having the parastyle very small to indistinct. These three taxa do not differ in development of the parastyle.

***Eomaia* and *Sinodelphys*.** Both of these taxa are known from reasonably complete, but much flattened skeletons from the Barremian Yixian Formation of the Dawangzhangzi locality in Liaoning, China (Ji *et al*. 2002; Luo *et al*. 2003). The postcanine dental formula of *Eomaia scansoria* Ji *et al*., 2002 was interpreted as P1-5, M1-3/p1-5, m1-3, and this taxon was diagnosed as differing from *Prokennalestes* in having a larger metastylar and metaconal region on M3 (Ji *et al*. 2002). According to the interpretations of Ji *et al*. (2002), *Eomaia* is furthermore distinct from *Prokennalestes* in having a tall and trenchant nonmolariform P5 positioned below the infraorbital foramen and a very small P4, while in *Prokennalestes* P5 is lower and submolariform and P4 is tall, trenchant, and positioned below the infraorbital foramen (Kielan-Jaworowska & Dashzeveg 1989). If the original interpretation of the *Eomaia* upper dentition is not correct, the "last" molar with an unreduced metacone and metaconule would be M2, the tall trenchant premolar below the infraorbital foramen would be P4, and one of the small anterior premolars would be a milk tooth that has not been replaced. In all known early eutherians M3 has a reduced distal side, including the metacone and metaconule, which is functionally correlated with the lack of a lower molar posterior to m3; a similar structure of M3 would be expected for *Eomaia* if it has three lower molars.

A very similar pattern for the posterior cheek tooth dentition is present in *Sinodelphys szalayi* Luo *et al*., 2003: a tall trenchant P4 below the infraorbtal foramen, a submolariform P5, a simple ultimate lower premolar, and three upper and lower molars. Luo *et al*. (2003) interpreted *Sinodelphys* as having four upper and three lower molars, but the reasons for this interpretation were not given. It is important to note that there are no Cretaceous therian mammals that have a different number of upper and lower molars. We think it very possible that the basal therians *Eomaia*, *Prokennalestes* and *Sinodelphys* had a similar pattern of posterior cheek teeth as outlined above, apparently inherited from a common ancestor, and a common postcanine dental formula: P1-5/p1-5, M1-3/m1-3. In the single specimen of *Sinodelphys* only four lower premolars are preserved, but a large diastema between the first and the second preserved premolars is present, which may have housed another premolar (p2). Even if there are no alveoli for such a tooth, it can be ontogenetically lost and its alveoli closed as demonstrated in some specimens of zhelestids and *Gypsonictops*. If this surmise is correct, p2 would have been where the diastema occurs between p1 and p3, as in the upper jaw of this specimen P2 is separated from P1 and P3.

Neither *Eomaia* nor *Sinodelphys* were included in the phylogenetic analysis of Rougier *et al*. (2004). These are also not included in our analysis, because we had no opportunity to study these specimens firsthand and some published interpretations of dental morphology seem to be open to interpretation. Until photographs and illustrations of the upper dentition are made available, especially for *Eomaia*, the true nature of the dental formula of these taxa must remain equivocal.

***Zhelestes* and *Aspanlestes*.** Rougier *et al*. (2004) used both of these taxa from the Turonian Bissekty Formation of Dzharakuduk in the Kyzylkum Desert, Uzbekistan as a terminal taxon representing the Zhelestidae. The zhelestids from Dzharakuduk are now represented by numerous additional specimens, including cranial fragments, currently under study by us (Ekdale *et al*. 2004; Archibald & Averianov 2005). We restrict this terminal taxon to the better-known *Aspanlestes* because of some variation between zhelestid taxa (e.g. the upper and lower canine is single-rooted in *Zhelestes* but double-rooted or bifurcate in *Aspanlestes*).

Phylogenetic analysis

The data matrix (Appendix 2) was analyzed with PAUP, version 4.0b10 (Swofford 2002) using the heuristic search algorithm (random addition, 1000 replications). All multistate characters were ordered as in the analysis by Rougier *et al*. (2004). The PAUP analysis produced 7045 equally most parsimonious trees with a tree length of 329, a consistency index of 0.42 and a retention index 0.69. The strict consensus tree is poorly resolved, revealing only four clades: (1) *Deltatheridium* + *Deltatheroides* + *Sulestes*; (2) *Didelphodon* + *Eodelphis*; (3) *Jaskhadelphys* + (*Andinodelphis* + *Pucadelphis*); and (4) *Asioryctes* + *Kennalestes*. To increase resolution a successive reweighing was performed based on weights from rescaled consistency index. The reweighed matrix was run in PAUP using the same options as in the previous analysis. In this analysis 46 equally most parsimonious trees were found with a tree length of 127, a consistency index of 0.59, and a retention index 0.82. The strict consensus of these trees is shown in Fig. 8 and the apomorphies are cited in Appendix 3. A bootstrap analysis using 10,000 replicates in the "fast" stepwise-addition setting did not recover many values over 70, which is usually taken to indicate strong support. All bootstrap values for clades over 50 are given as bold numbers in parentheses following the appropriate node in Appendix 3.

This resulting cladogram is similar in many respects to the cladogram obtained by Rougier *et al*. (2004, fig. 8). Three major metatherian clades are recognised: Deltatheroida, Boreometatheria and Notometatheria (Fig. 8). The principal novelties of our analysis are the position of the North American Early Cretaceous *Montanalestes* and *Pappotherium* as stem tribosphenic mammals, and *Holoclemensia* as a stem eutherian. Another significant change is the removal of the Mongolian unnamed *Deltatheroides*-like Guriliin Tsav taxon from the proximity of the Stagodontidae to basal Boreometatheria.

Therian dental evolution near the Metatherian-Eutherian dichotomy

Interpretation of the transformation of the dental formula from basal tribosphenic mammals to eutherians and metatherians is highly uncertain because of a lack of adequate fossils with complete tooth rows preserved (see reviews of the problem in Ziegler 1971; Fox 1975; McKenna 1975; Bown & Kraus 1979; Prothero 1981; Slaughter 1981; Novacek 1986). Here we summarize briefly our view of this transition, which included four major evolutionary events (Fig. 9):

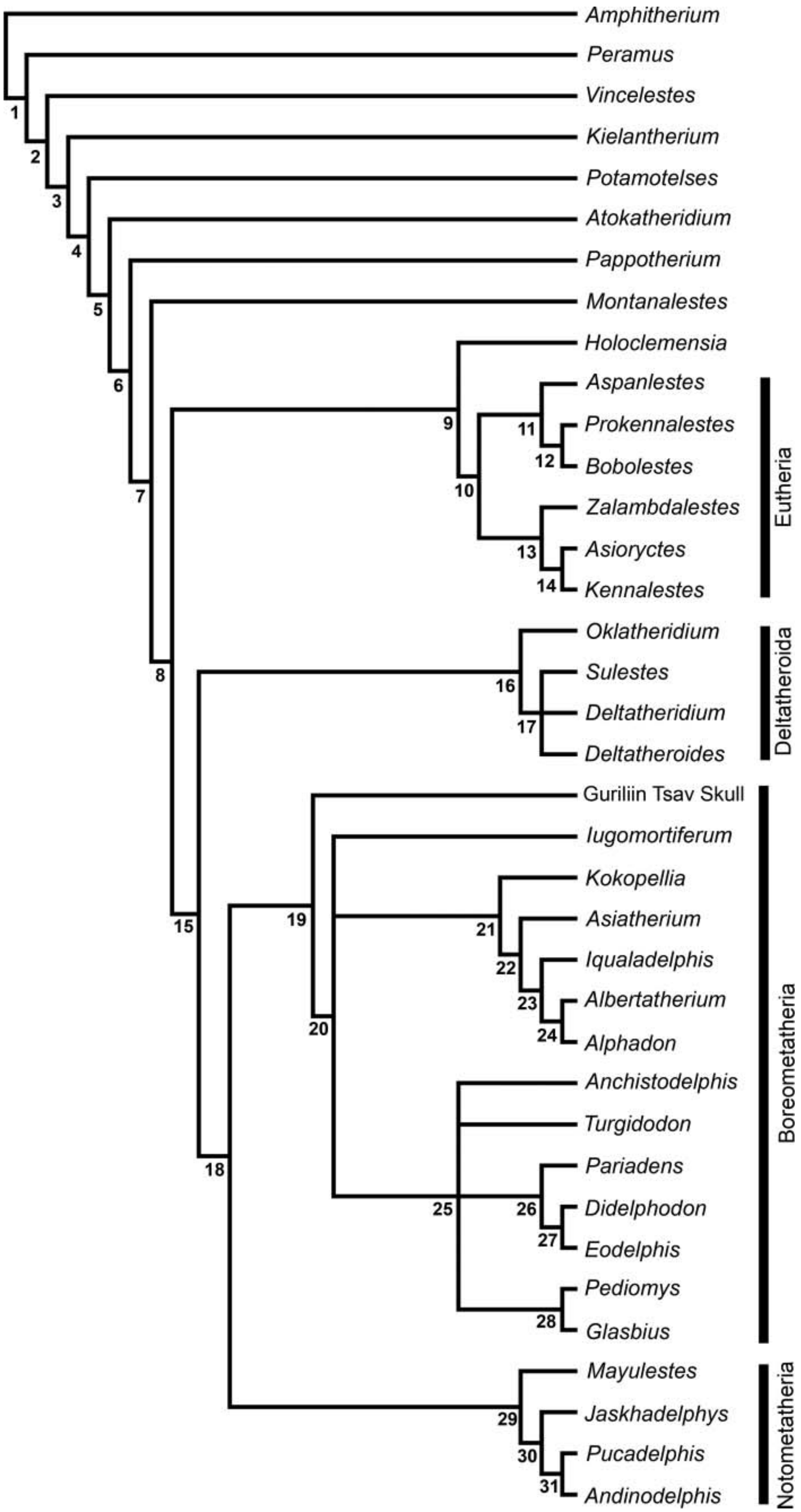

Figure 8. Strict consensus tree of 46 most parsimonious trees produced by PAUP. Apomorphies for numbered nodes and terminal taxa are listed in Appendix 3.

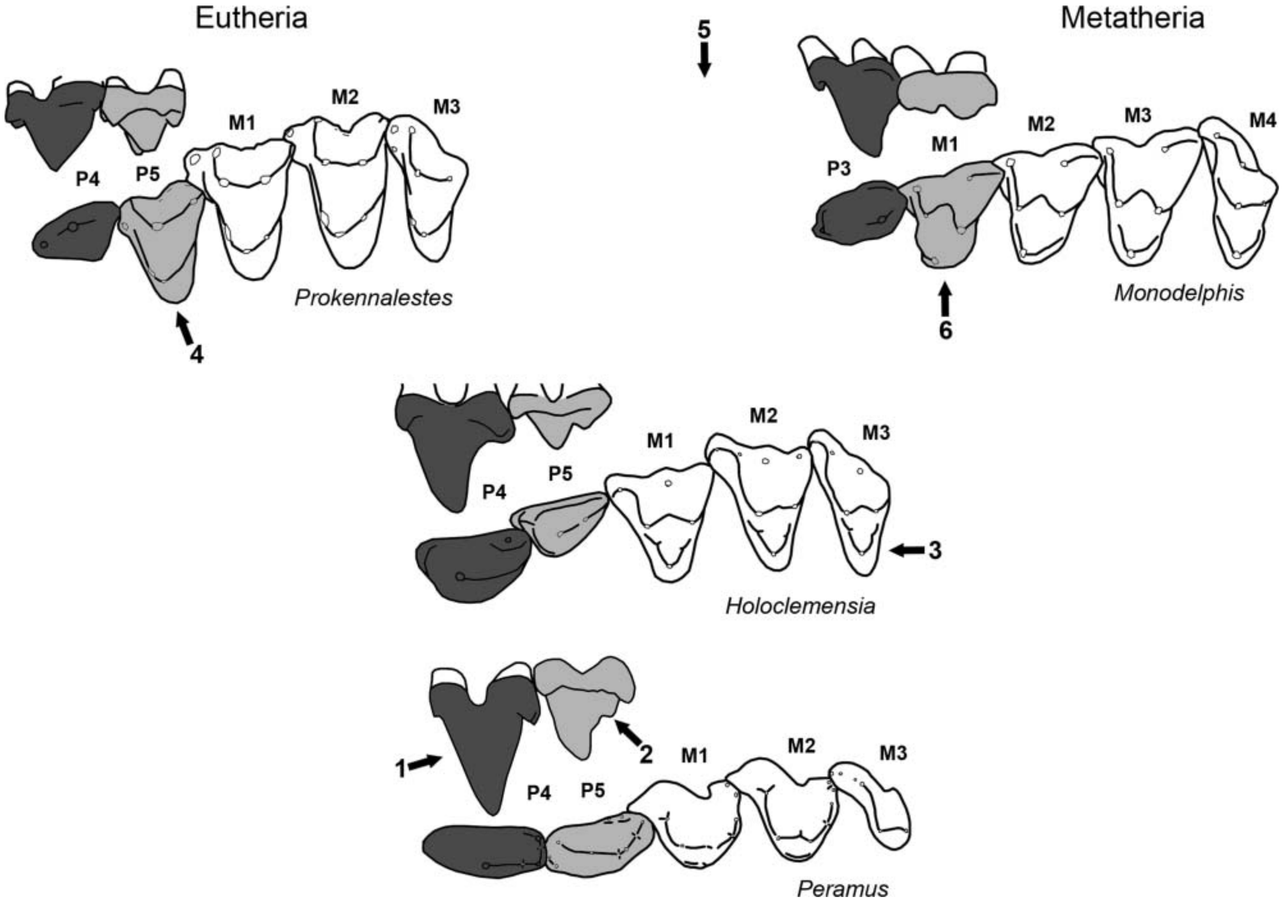

Figure 9. Diagram showing suggested homology of tooth positions and dental formula differentiation in pretribosphenic and early tribosphenic mammals. Five posterior left cheek teeth are shown in occlusal view and two anterior of them also in labial view (not to scale). Homologous premolar tooth positions are marked by different grey colors. Numbered arrows indicate acquisition of these characters: (1) tall trenchant ("sectorial") P4; (2) metacone on P5; (3) protocone on upper molars; (4) protocone on P5; (5) lost of P1 tooth position; (6) lost of replacement in P5 locus. *Peramus* is after Clemens & Mills (1971), *Holoclemensia* is after Butler (1978, various figures: P4 is SMP-SMU 61948, P5 is CNHM PM 931, M1 is reconstructed based on CNHM PM 886 and 1000, M2 is based on SMP-SMU 61947, and M3 is SMPU-SMU 62099), *Prokennalestes* is after Kielan-Jaworowska & Dashzeveg (1989), and *Monodelphis* is after Reig *et al*. (1987).

(1) Presence of a P1-5, M1-3 postcanine dental formula in derived pretribosphenic mammals exemplified by *Peramus* (synapomorphy of Zatheria McKenna, 1975). In the evolutionary lineage leading to *Peramus* the number of molars was gradually reduced from six-seven (*Amphitherium*) to five (*Nanolestes*) and four (*Arguimus*), but all of these taxa had five premolars (Butler & Clemens 2001; Martin 2002; Lopatin & Averianov 2006a). The upper premolars are not known in stem zatherians. In *Peramus* the two last upper premolars are highly distinctive: P4 is tall and trenchant ("sectorial"), with a distinct distolabial cingular cusp and P5 has an additional cusp, metacone, distal to the main cusp, paracone (McKenna 1975) (characters 1 and 2 on Fig. 8).

(2) Acquisition of protocones on upper molars (character 3 on Fig. 8). While *Peramus* shows a cingulum in the presumptive position of a protocone, it is among Trinity therians that we first see upper molars with a fully developed protocone (*Holoclemensia*). In the Trinity therian sample there are isolated teeth that greatly resemble the posterior upper premolars seen in *Peramus*, one type a tall trenchant P4 with a distolabial cingular cusp and another with a lower crowned P5 with a metacone. These morphological similarities are sufficient enough to argue for the homology between these teeth and the posterior premolars of *Peramus* (Fig. 9). Given this identification of these posterior premolars in *Holoclemensia* it is equally likely that this taxon also had three molars as in *Peramus*, not four as suggested by Butler (1978).

(3) Acquisition of protocone on P5 (character 4 in Fig. 8). This is apparently the only nonhomoplasic dental synapomorphy for Eutheria.

(4) Loss of P1 locus; loss of replacement in P5 locus, with molariform DP5 becoming "M1;" dental formula becomes P1-3 M1-4 (characters 5 and 6 on Fig. 9). As depicted in Fig. 8, the metatherian P3, M1, M2, M3, and M4 are homologues to the ancestral therian (and eutherian) P4, DP5, M1, M2 and M3, respectively (McKenna 1975). This homology is supported by: the metatherian P3 and the eutherian P4 being the tallest upper premolars and this tooth is always placed below the infraorbital foramen (as in *Peramus*), the metatherian M1/m1 and eutherian DP5/dp5 always being the smallest of the remaining molars in basal metatherians and basal eutherians, and the metatherian M4 and the eutherian M3 having a reduced metacone and metastylar area. Because the acquisition of four molars in metatherians is a derived character, it reiterates the argument given in the second dental event that *Holoclemensia* had the ancestral state of only three molars with a tall trenchant permanent P4 that is homologous to the tall trenchant permanent P3 of metatherians and a lower crowned P5 with a metacone (but no protocone) homologous to the permanent P5 that has been lost in metatherians.

We think that the scheme presented above explains most parsimoniously the transformation of the dental formula and homology of the posterior check tooth loci leading up to the Eutheria-Metatheria dichotomy. The only taxon that does not easily fit this scheme is *Kielantherium*, which had four or five premolars, four molars and an incipient protocone (Lopatin & Averianov 2006b, 2007). There are two possible hypotheses explaining its phylogenetic position.

First, *Kielantherium* is a stem zatherian that branched prior to *Peramus* from an ancestor with four molars, such as *Arguimus*. This hypothesis implies that protocone of *Kielantherium* was developed independently of other therians, which would not be a great surprise as we now know a number of independent attempts to produce tribosphenic-like dentition (e.g. Luo *et al*. 2007b; Averianov & Lopatin 2008).

Second, *Kielantherium* is a stem metatherian that branched after *Peramus* and had already suppressed replacement in the P5/p5 locus (consequently, *Kielantherium* must have only four premolars). This hypothesis implies an early divergence of eutherian and metatherian lineages at a stage when the protocone was still relatively small as in *Kielantherium*. It further implies that Trinity therians that had evolved a better-developed protocone but still replaced at the P5/p5 locus are stem eutherians, not stem metatherians. This second hypothesis is supported by our phylogenetic analysis (see previous section). These two hypotheses can be also easily tested by discovery of more complete *Kielantherium* specimens: if they have five premolars this would support the first hypothesis and four premolars would support the second hypothesis.

Acknowledgements

We thank Sandrine Ladevèze (Muséum National d'Histoire Naturelle, Paris), Richard Cifelli (University of Oklahoma, Norman), John Wible and Zhe-Xi Luo (both from Carnegie Museum of Natural History, Pittsburgh) for reading an earlier version of this paper and for providing suggestions. We thank Guillermo Rougier (University of Louisville, Louisville) and an anonymous reviewer for reviewing the paper. The continued cooperation of the Zoological Institute, National Academy of Sciences of Uzbekistan, notably D. A. Azimov and Y. A. Chikin, is much appreciated. We thank the URBAC expedition members A. V. Abramov, G. O. Cherepanov, I. G. Danilov, S. Dominguez, C. King, N. J. Morris, C. Redman, A. S. Resvyi, C. Skrabec, P. P. Skutschas, H.-D. Sues, E. V. Syromyatnikova and D. W. Ward for their myriad field help and scientific expertise. AA thanks Andrei Bochkov (Zoological Institute, St Petersburg) for consultations. EE thanks Jen Olori (University of Texas, Austin) for helpful comments. The financial support of the National Geographic Society (5901-97 and 6281-98), the National Science Foundation (EAR-9804771 and 0207004), the Navoi Mining and Metallurgy Combinat, the Civilian Research and Development Foundation (RU-G1-2571-ST-04 and RUB1-2860-ST-07) and the Russian Fund of Basic Research (07-04-91110-AFGIRa) are gratefully acknowledged. The work of AA was also supported by the President's of Russia grant MD 255.2003.04, by the Russian Fund of Basic Research grants 04-04-49113, 04-04-49637, and 07-04-00393 and by the Russian Science Support Foundation.

References

Archibald, J. D. 1982. A study of Mammalia and geology across the Cretaceous-Tertiary boundary in Garfield County, Montana. *University of California Publications in Geological Sciences*, **122**, 1–286.

Archibald, J. D. & **Averianov, A. O.** 2005. Mammalian faunal succession in the Cretaceous of the Kyzylkum Desert. *Journal of Mammalian Evolution*, **12**, 9–22.

Archibald, J. D. & **Averianov, A. O.** 2007. Zhelestids: stem eutherians or basal laurasiatherians, but no evidence for placental orders in the Cretaceous. *Journal of Vertebrate Paleontology*, **27**, 41A.

Averianov, A. O. 1997. New Late Cretaceous mammals of southern Kazakhstan. *Acta Palaeontologica Polonica*, **42**, 243–256.

Averianov, A. O. 2000. Mammals from the Mesozoic of Kirgizstan, Uzbekistan, Kazakhstan and Tadzhikistan. Pp. 627–652 in M. J. Benton, M. A. Shishkin, D. M. Unwin & E. N. Kurochkin (eds) *The Age of Dinosaurs in Russia and Mongolia*. Cambridge University Press, Cambridge.

Averianov, A. O. & **Archibald, J. D.** 2003. Mammals from the Upper Cretaceous Aitym Formation, Kyzylkum Desert, Uzbekistan. *Cretaceous Research*, **24**, 171–191.

Averianov, A. O. & **Archibald, J. D.** 2005. Mammals from the mid-Cretaceous Khodzhakul Formation, Kyzylkum Desert, Uzbekistan. *Cretaceous Research*, **26**, 593–608.

Averianov, A. O. & **Kielan-Jaworowska, Z.** 1999. Marsupials from the Late Cretaceous of Uzbekistan. *Acta Palaeontologica Polonica*, **44**, 71–81.

Averianov, A. O. & **Lopatin, A. V.** 2008. "Protocone" in a pretribosphenic mammal and upper dentition of tinodontid "symmetrodontans." *Journal of Vertebrate Paleontology*, **28**, 548–552.

Averianov, A. O. & **Skutschas, P. P.** 1999. Phylogenetic relationships within basal tribosphenic mammals. *Proceedings of the Zoological Institute of the Russian Academy of Sciences*, **281**, 55–60.

Benton, M. J. 2000. Conventions in Russian and Mongolian paleontological literature. Pp. xvi–xxxix in M. J. Benton, M. A. Shishkin, D. M. Unwin & E. N. Kurochkin (eds) *The Age of Dinosaurs in Russia and Mongolia*. Cambridge University Press, Cambridge.

Bown, T. M. & **Kraus, M. J.** 1979. Origin of the tribosphenic molar and metatherian and eutherian dental formulae. Pp. 162–171 in J. A. Lillegraven, Z. Kielan-Jaworowska & W. A. Clemens (eds) *Mesozoic Mammals: the First Two-Thirds of Mammalian History.* University of California Press, Berkeley.

Butler, P. M. 1978. A new interpretation of the mammalian teeth of tribosphenic pattern from the Albian of Texas. *Breviora*, **446**, 1–27.

Butler, P. M. & **Clemens, W. A.** 2001. Dental morphology of the Jurassic holotherian mammal *Amphitherium*, with a discussion of the evolution of mammalian post-canine dental formulae. *Palaeontology*, **44**, 1–20.

Butler, P. M. & **Kielan-Jaworowska, Z.** 1973. Is *Deltatheridium* a marsupial? *Nature*, **245**, 105–106.

Chester, S. G. B., **Sargis, E. J.**, **Szalay, F. S.**, **Archibald, J. D.** & **Averianov, A. O.** 2007. Functional analysis of mammalian humeri from the Late Cretaceous of Uzbekistan. *Journal of Vertebrate Paleontology*, **27**, 58A.

Cifelli, R. L. 1990. Cretaceous mammals of southern Utah. III. Therian mammals from the Turonian (early Late Cretaceous). *Journal of Vertebrate Paleontology*, **10**, 332–345.

Cifelli, R. L. 1993a. Early Cretaceous mammal from North America and the evolution of marsupial dental characters. *Proceedings of the National Academy of Sciences*, **90**, 9413–9416.

Cifelli, R. L. 1993b. Theria of metatherian-eutherian grade and the origin of marsupials. Pp. 205–215 in F. S. Szalay, M. J. Novacek & M. C. McKenna (eds) *Mammal Phylogeny: Mesozoic Differentiation, Multituberculates, Monotremes, Early Therians, and Marsupials*. Springer-Verlag, New York.

Cifelli, R. L. 1999. Tribosphenic mammal from the North American Early Cretaceous. *Nature*, **401**, 363–366.

Cifelli, R. L. & **Muizon, C. de** 1997. Dentition and jaw of *Kokopellia juddi*, a primitive marsupial or near marsupial from the medial Cretaceous of Utah. *Journal of Mammalian Evolution*, **4**, 241–258.

Clemens, W. A. 1966. Fossil mammals of the type Lance Formation Wyoming. Part II. Marsupialia. *University of California Publications in Geological Sciences*, **62**, 1–122.

Clemens, W. A. & **Mills, J. R. E.** 1971. Review of *Peramus tenuirostris* Owen (Eupantotheria Mammalia). *Bulletin of the British Museum (Natural History), Geology Series*, **20**, 89–113.

Crompton, A. W. 1971. The origin of the tribosphenic molar. Pp. 65–87 in D. M. Kermack & K. A. Kermack (eds) *Early Mammals*. Zoological Journal of the Linnean Society, London.

Dashzeveg, D. 1975. New primitive therian from the Early Cretaceous of Mongolia. *Nature*, **256**: 402–403.

Davis, B. M., **Cifelli, R. L.** & **Kielan-Jaworowska, Z.** 2008. Earliest evidence of Deltatheroida (Mammalia: Metatheria) from the Early Cretaceous of North America. Pp. 3–24 in E. J. Sargis & M. Dagosto (eds) *Mammalian Evolutionary Morphology. A Tribute to Frederick S. Szalay*. Vertebrate Paleobiology and Paleoanthropology Series, Springer, Dordrecht.

Davis, B. & **Davies, K.** 2005. First vertebrate fossils from the Eagle Formation (Upper Santonian), north central Montana. *Journal of Vertebrate Paleontology*, **25**, 50A.

Eaton, J. G. 1993. Therian mammals from the Cenomanian (Upper Cretaceous) Dakota Formation, southwestern Utah. *Journal of Vertebrate Paleontology*, **13**, 105–124.

Eaton, J. G. 2006. Santonian (Late Cretaceous) mammals from the John Henry Member of the Straight Cliffs Formation, Grand Staircase-Escalante National Monument, Utah. *Journal of Vertebrate Paleontology*, **26**, 446–460.

Ekdale, E. G., **Archibald, J. D.** & **Averianov, A. O.** 2004. Petrosal bones of placental mammals from the Late Cretaceous of Uzbekistan. *Acta Palaeontologica Polonica*, **49**, 161–176.

Fox, R. C. 1972. A primitive therian mammal from the Upper Cretaceous of Alberta. *Canadian Journal of Earth Sciences*, **9**, 1479–1494.

Fox, R. C. 1974. *Deltatheroides*-like mammals from the Upper Cretaceous of North America. *Nature*, **249**, 392.

Fox, R. C. 1975. Molar structure and function in the Early Cretaceous mammal *Pappotherium*: Evolutionary implications for Mesozoic Theria. *Canadian Journal of Earth Sciences*, **12**, 412–442.

Fox, R. C. 1980. *Picopsis pattersoni*, n. gen. and sp., an unusual therian from the Upper Cretaceous of Alberta, and the classification of primitive tribosphenic mammals. *Canadian Journal of Earth Sciences*, **17**, 1489–1498.

Fox, R. C. 1982. Evidence of new lineage of tribosphenic therians (Mammalia) from the Upper Cretaceous of Alberta, Canada. *Géobios, Mémoire Spécial*, **6**, 169–175.

Fox, R. C. & **Naylor, B. G.** 2006. Stagodontid marsupials from the Late Cretaceous of Canada and their systematic and functional implications. *Acta Palaeontologica Polonica*, **51**, 13–36.

Gregory, W. K. & **Simpson, G. G.** 1926. Cretaceous mammal skulls from Mongolia. *American Museum Novitates*, **225**, 1–20.

Hiiemae, K. M. & **Jenkins, F. A. jnr** 1969. The anatomy and internal architecture of the muscles of mastication in *Didelphis marsupialis*. *Postilla*, **140**, 1–49.

Horovitz, I. 2000. The tarsus of *Ukhaatherium nessovi* (Eutheria, Mammalia) from the Late Cretaceous of Mongolia: an appraisal of the evolution of the ankle in basal therians. *Journal of Vertebrate Paleontology*, **20**, 547–560.

Huxley, T. H. 1880. On the application of the laws of evolution to the arrangement of the Vertebrata and more particularly of the Mammalia. *Proceedings of the Zoological Society of London*, **43**, 649–662.

Ji, Q., **Luo, Z.-X.**, **Yuan, C.-X.** & **Tabrum, A. R.** 2006. A swimming mammaliaform from the Middle Jurassic and ecomorphological diversification of early mammals. *Science*, **311**, 1123–1127.

Ji, Q., **Luo, Z.-X.**, **Yuan, C.-X.**, **Wible, J. R.**, **Zhang, J.-P.** & **Georg, J. A.** 2002. The earliest known eutherian mammal. *Nature*, **416**, 816–822.

Kielan-Jaworowska, Z. 1975. Evolution of the therian mammals in the Late Cretaceous of Asia. Part I. Deltatheridiidae. *Palaeontologia Polonica*, **33**, 103–132.

Kielan-Jaworowska, Z. 1982. Marsupial-placental dichotomy and paleogeography of Cretaceous Theria. Pp. 367–383 in E. M. Gallitelli (ed.) *Palaeontology, Essential of Historical Geology*. S.T.E.M. Mucci, Modena.

Kielan-Jaworowska, Z. & **Cifelli, R. L.** 2001. Primitive boreosphenidan mammal (?Deltatheroida) from the Early Cretaceous of Oklahoma. *Acta Palaeontologica Polonica*, **46**, 377–391.

Kielan-Jaworowska, Z. & **Dashzeveg, D.** 1989. Eutherian mammals from the Early Cretaceous of Mongolia. *Zoologica Scripta*, **18**, 347–355.

Kielan-Jaworowska, Z. & **Nessov, L. A.** 1990. On the metatherian nature of the Deltatheroida, a sister group of the Marsupialia. *Lethaia*, **23**, 1–10.

Kielan-Jaworowska, Z., **Eaton, J. G.** & **Bown, T. M.** 1979. Theria of metatherian-eutherian grade. Pp. 182–191 in J. A. Lillegraven, Z. Kielan-Jaworowska & W. A. Clemens (eds) *Mesozoic Mammals: The First Two-thirds of Mammalian History.* University of California Press, Berkeley.

Kielan-Jaworowska, Z., **Novacek, M. J.**, **Trofimov, B. A.** & **Dashzeveg, D.** 2000. Mammals from the Mesozoic of Mongolia. Pp. 573–626 in M. J. Benton, M. A. Shishkin, D. M. Unwin & E. N. Kurochkin (eds) *The Age of Dinosaurs in Russia and Mongolia*. Cambridge University Press, Cambridge.

Kielan-Jaworowska, Z., **Cifelli, R. L.** & **Luo, Z.-X.** 2004. *Mammals from the Age of Dinosaurs: Origins, Evolution, and Structure*. Columbia University Press, New York, 630 pp.

Li, C.-K., **Setoguchi, T.**, **Wang, Y.-Q.**, **Hu, Y.-M.** & **Chang, Z.-L.** 2005. The first record of "eupantotherian" (Theria, Mammalia) from the late Early Cretaceous of western Liaoning, China. *Vertebrata PalAsiatica*, **43**, 245–255.

Li, G. & **Luo, Z.-X.** 2006. A Cretaceous symmetrodont therian with some monotreme-like postcranial features. *Nature*, **439**, 195–200.

Linnaeus, C. 1758. *Systema naturae per regna tria naturae, secundum classes, ordines, genera, species, cum characteribus, differentiis, synonymis, locis. Vol. 1: Regnum animale*. Editio decima, reformata. Laurentii Salvii, Stockholm, 824 pp.

Lopatin, A. V. & **Averianov, A. O.** 2006a. Revision of a pretribosphenic mammal *Arguimus* from the Early Cretaceous of Mongolia. *Acta Palaeontologica Polonica*, **51**, 339–349.

Lopatin, A. V. & **Averianov, A. O.** 2006b. An aegialodontid upper molar and the evolution of mammal dentition. *Science*, **313**, 1092.

Lopatin, A. V. & **Averianov, A. O.** 2007. *Kielantherium*, a basal tribosphenic mammal from the Early Cretaceous of Mongolia, with new data on the aegialodontid dentition. *Acta Palaeontologica Polonica*, **52**, 441–446.

Luo, Z.-X. & **Wible, J. R.** 2005. A Late Jurassic digging mammal and early mammalian diversification. *Science*, **308**, 103–107.

Luo, Z.-X., **Chen, P.**, **Li, G.** & **Chen, M.** 2007a. A new eutriconodont mammal and evolutionary development in early mammals. *Nature*, **446**, 288–293.

Luo, Z.-X., **Ji, Q.** & **Yuan, C.-X.** 2007b. Convergent dental adaptations in pseudo-tribosphenic and tribosphenic mammals. *Nature*, **450**, 93–97.

Luo, Z.-X., **Kielan-Jaworowska, Z.** & **Cifelli, R. L.** 2002. In quest for a phylogeny of Mesozoic mammals. *Acta Palaeontologica Polonica*, **47**, 1–78.

Luo, Z.-X., **Ji, Q.**, **Wible, J. R.** & **Yuan, C.-X.** 2003. An Early Cretaceous tribosphenic mammal and metatherian evolution. *Science*, **302**, 1934–1940.

Martin, T. 2002. New stem-line representatives of Zatheria (Mammalia) from the Late Jurassic of Portugal. *Journal of Vertebrate Paleontology*, **22**, 332–348.

McKenna, M. C. 1975. Towards a phylogenetic classification of the Mammalia. Pp. 21–46 in W. P. Luckett & F. S. Szalay (eds) *Phylogeny of the Primates*. Plenum Press, New York.

McKenna, M. C. & **Bell, S. K.** 1997. *Classification of Mammals Above the Species Level*. Columbia University Press, New York, 631 pp.

McKenna, M. C., **Mellett, J. S.** & **Szalay, F. S.** 1971. Relationships of the Cretaceous mammal *Deltatheridium*. *Journal of Paleontology*, **45**, 441–442.

Meng, J., **Hu, Y.-M.**, **Wang, Y.**, **Wang, X.** & **Li, C.-K.** 2006. A Mesozoic gliding mammal from northeastern China. *Nature*, **444**, 889–893.

Muizon, C. de 1994. A new carnivorous marsupial from the Palaeocene of Bolivia and the problem of marsupial monophyly. *Nature*, **370**, 208–211.

Muizon, C., de & **Cifelli, R. L.** 2001. A new basal "didelphoid" (Marsupialia, Mammalia) from the early Paleocene of Tiupampa (Bolivia). *Journal of Vertebrate Paleontology*, **21**, 87–97.

Nessov, L. A. 1981. [Cretaceous salamanders and frogs of Kyzylkum Desert]. *Trudy Zoologicheskogo Instituta AN SSSR*, **101**, 57–88. [In Russian]

Nessov, L. A. 1982. [The most ancient mammals of the USSR]. *Ezhegodnik Vsesoyuznogo Paleontologicheskogo Obshchestva*, **25**, 228–242. [In Russian]

Nessov, L. A. 1985a. [New mammals from the Cretaceous of Kyzylkum]. *Vestnik Leningradskogo Universiteta, Seriya 7*, **17**, 8–18. [In Russian]

Nessov, L. A. 1985b. [Rare bony fishes, terrestrial lizards and mammals from the zone of estuaries and coastal plains of the Cretaceous of Kyzylkum]. *Ezhegodnik Vsesoyuznogo Paleontologicheskogo Obshchestva*, **28**, 199–219. [In Russian]

Nessov, L. A. 1987. [Results of search and study of Cretaceous and early Paleogene mammals on the territory of the USSR]. *Ezhegodnik Vsesoyuznogo Paleontologicheskogo Obshchestva*, **30**, 199–218. [In Russian]

Nessov, L. A. 1993. [New Mesozoic mammals of Middle Asia and Kazakhstan and comments about evolution of theriofaunas of Cretaceous coastal plains of Asia]. *Trudy Zoologicheskogo Instituta RAN*, **249**, 105–133. [In Russian]

Nessov, L. A. 1997. *[Cretaceous Nonmarine Vertebrates of Northern Eurasia]* (Posthumous edition by L. B. Golovneva and A. O. Averianov). Izdatel'stvo Sankt-Peterburgskogo Universiteta, St Petersburg, 218 pp. [In Russian]

Nessov, L. A. & **Kielan-Jaworowska, Z.** 1991. Evolution of the Cretaceous Asian therian mammals. Pp. 51–52 in Z. Kielan-Jaworowska, N. Heintz & H.-A. Nakrem (eds) *Fifth Symposium on Mesozoic Terrestrial Ecosystems and Biota*. Extended Abstracts. Contributions from the Paleontological Museum, University of Oslo.

Nessov, L. A., **Sigogneau-Russell, D.** & **Russell, D. E.** 1994. A survey of Cretaceous tribosphenic mammals from Middle Asia (Uzbekistan, Kazakhstan and Tajikistan), of their geological setting, age and faunal environment. *Palaeovertebrata*, **23**, 51–92.

Nixon, K. C. 1999. *Winclada (Beta) version 0.9.9*. Software published by the author, Ithaca, New York. Available on-line at http://www.cladistics.org/tnt.html.

Novacek, M. J. 1986. The primitive eutherian dental formula. *Journal of Vertebrate Paleontology*, **6**, 191–196.

Prothero, D. R. 1981. New Jurassic mammals from Como Bluff, Wyoming, and the interrelationships of non-tribosphenic Theria. *Bulletin of the American Museum of Natural History*, **167**, 281–325.

Reig, O. A., **Kirsch, J. A. W.** & **Marshall, L. G.** 1987. Systematic relationships of the living and Neocenozoic American “opossum-like” marsupials (suborder Didelphimorphia), with comments on the classification of these and of the Cretaceous and Paleogene New World and European metatherians. Pp. 1–89 in M. Archer (ed.) *Possums and Opossums: Studies in Evolution*. Surrey Beatty and Sons and the Royal Zoological Society of New South Wales, Sydney.

Rougier, G. W., **Wible, J. R.** & **Novacek, M. J.** 1998. Implications of *Deltatheridium* specimens for early marsupial history. *Nature*, **396**, 459–463.

Rougier, G. W., **Wible, J. R.** & **Novacek, M. J.** 2004. New specimen of *Deltatheroides cretacicus* (Metatheria, Deltatheroida) from the Late Cretaceous of Mongolia. *Bulletin of the Carnegie Museum of Natural History*, **36**, 245–266.

Sánchez-Villagra, M. R. & **Smith, K. K.** 1997. Diversity and evolution of the marsupial mandibular angular process. *Journal of Mammalian Evolution*, **4**, 119–144.

Segall, W. 1970. Morphological parallelisms of the bulla and auditory ossicles in some insectivores and marsupials. *Fieldiana: Zoology*, **51**, 169–205.

Slaughter, B. H. 1981. The Trinity therians (Albian, mid-Cretaceous) as marsupials and placentals. *Journal of Paleontology*, **55**, 682–683.

Swofford, D. L. 2002. *PAUP*. Phylogenetic Analysis Using Parsimony (*and Other Methods). Version 4.0*. Sinauer Associates, Sunderland.

Szalay, F. S. & **McKenna, M. C.** 1971. Beginning of the age of mammals in Asia: The Late Paleocene Gashato fauna, Mongolia. *Bulletin of the American Museum of Natural History*, **144**, 269–318.

Szalay, F. S. & **Sargis**, **E. J.** 2006. Cretaceous Therian Tarsals and the Metatherian-Eutherian Dichotomy. *Journal of Mammalian Evolution*, **13**, 171–210.

Van Valen, L. M. 1966. Deltatheridia, a new order of mammals. *Bulletin of the American Museum of Natural History*, **132**, 1–126.

Van Valen, L. M. 1974. *Deltatheridium* and marsupials. *Nature* **248**, 165–166.

Wible, J. R. 2003. On the cranial osteology of the short-tailed opossum *Monodelphis brevicaudata* (Didelphidae, Marsupialia). *Annals of Carnegie Museum*, **72**, 137–202.

Wible, J. R., **Rougier, G. W.**, **Novacek, M. J.** & **McKenna, M. C.** 2001. Earliest eutherian ear region: a petrosal referred to *Prokennalestes* from the Early Cretaceous of Mongolia. *American Museum Novitates*, **3322**, 1–44.

Wible, J. R., **Novacek, M. J.** & **Rougier, G. W.** 2004. New data on the skull and dentition in the Mongolian Late Cretaceous eutherian mammal *Zalambdalestes*. *Bulletin of the American Museum of Natural History*, **281**, 1–144.

Wible, J. R., **Rougier, G. W.**, **Novacek, M. J.** & **Asher, R. J.** 2007. Cretaceous eutherians and Laurasian origin for placental mammals near the K/T boundary. *Nature*, **447**, 1003–1006.

Wood, C. B. 2000. Tooth enamel microstructure in *Deltatheridium* (Metatheria, Late Cretaceous of Mongolia), with comparison to some other Mesozoic mammals. *Bulletin of the Paleontological Society of Korea, Special Publication*, **4**, 127–152.

Ziegler, A. C. 1971. A theory of the evolution of therian dental formulas and replacement pattern. *Quarterly Review of Biology*, **46**, 226–249.

Appendix 1

List of characters used in the phylogenetic analysis

1. Number of postcanine tooth families: (0) eight or more; (1) seven or less.
2. Premolars: number: (0) five; (1) four; (2) three or fewer.
3. Premolars: cusp form: (0) sharp, uninflated; (1) inflated, with apical wear strongly developed.
4. Tall, trenchant premolar: (0) in ultimate premolar position; (1) in penultimate premolar position; (2) absent.
5. Molars: number: (0) more than four; (1) four; (2) three.
6. Molars: cusp form: (0) sharp, gracile; (1) inflated, robust.
7. Size of molars increasing posteriorly: (0) absent; (1) moderate posterior increase; (2) marked posterior increase.
8. Upper incisors: number: (0) five; (1) fewer than five.
9. Upper canine: number of roots: (0) two; (1) one.
10. Penultimate upper premolar: protocone: (0) absent; (1) small lingual bulge; (2) with an enlarged basin.
11. Penultimate upper premolar: number of roots: (0) two; (1) three.
12. Ultimate upper premolar: (0) simple; (1) molariform.
13. Upper molar shape: (0) as long as wide, or longer; (1) wider than long.
14. Upper molar outline in occlusal view: (0) does approach isosceles triangle; (1) does not approach isosceles triangle.
15. Upper molars: stylar shelf: (0) uniform in width, 50% or more of total transverse width; (1) uniform in width, but less than 50% of total transverse width; (2) reduced labial to paracone; (3) strongly reduced or absent.
16. Upper molars: deep ectoflexus: (0) present only on penultimate molar; (1) on penultimate and preceding molar; (2) strongly reduced or absent.
17. Upper molars: stylar cusp A: (0) distinct, but smaller than B; (1) subequal to or larger than B; (2) very small to indistinct.
18. Upper molars: preparastyle: (0) absent; (1) present.
19. Upper molars: stylar cusp B size relative to paracone: (0) smaller but distinct; (1) vestigial to absent; (2) subequal.
20. Upper molars: stylar cusp C: (0) absent; (1) present.

21. Upper molars: stylar cusp D: (0) absent; (1) smaller or subequal to B; (2) larger than B.
22. Upper molars: stylar cusp E: (0) directly lingual to D or D position; (1) distal to D; (2) small to indistinct.
23. Upper molars: preparacingulum: (0) absent; (1) interrupted between stylar margin and paraconule; (2) continuous.
24. Upper molars: metacone size relative to paracone: (0) noticeably smaller; (1) slightly smaller; (2) subequal to larger.
25. Upper molars: metacone position relative to paracone: (0) labial; (1) approximately at same level; (2) lingual.
26. Upper molars: metacone and paracone shape: (0) conical; (1) subtriangular, with labial face flat.
27. Upper molars: metacone and paracone bases: (0) adjoined; (1) separated.
28. Upper molars: centrocrista: (0) straight; (1) V-shaped.
29. Upper molars: salient postmetacrista: (0) weakly developed; (1) strongly developed, with paraconid enlarged and metaconid reduced on lower molars.
30. Upper molars: preprotocrista: (0) absent; (1) does not extend labially past base of paracone; (2) does extend labially past base of paracone (double rank prevallum/postvallid shearing).
31. Upper molars: postprotocrista: (0) absent; (1) does not extend labially past base of metacone; (2) does extend labially past base of metacone (double rank prevallum/postvallid shearing).
32. Upper molars: conules: (0) absent; (1) small, without cristae; (2) strong, labially placed, with wing-like cristae.
33. Upper molars: protocone 1: (0) lacking; (1) small, without trigon basin; (2) small, with distinct trigon basin; (3) somewhat expanded anteroposteriorly; (4) with posterior portion expanded.
34. Upper molars: protocone 2: (0) absent; (1) not procumbent; (2) procumbent.
35. Upper molars: protocone 3: (0) absent; (1) low; (2) tall, approaching para- and/or metacone height.
36. Upper molars: protocingula: (0) protocone absent; (1) protocone present, protocingula absent; (2) pre- and/or postcingulum present.
37. Upper molars: lingual root position: (0) supporting paracone; (1) supporting trigon.
38. Penultimate upper molar: metastylar area: (0) large; (1) reduced.
39. Ultimate upper molar: width relative to penultimate upper molar: (0) subequal; (1) smaller.
40. Lower incisors: number: (0) four; (1) fewer than four.
41. Staggered lower incisor: (0) absent; (1) present.
42. Lower canine: number of roots: (0) two; (1) one.
43. First lower premolar: (0) oriented in line with jaw axis; (1) oblique.
44. Second lower premolar: (0) smaller than third premolar; (1) larger.
45. Ultimate lower premolar: (0) simple; (1) complex, with a partial trigonid and/or talonid; (2) molariform.
46. Lower molars: trigonid configuration: (0) open, with paraconid anteromedial; (1) more acute, with paraconid more posteriorly placed; (2) anteroposteriorly compressed.
47. Lower molars: protoconid height: (0) tallest cusp on trigonid; (1) subequal to para- and/or metaconid.
48. Lower molars: paraconid height relative to metaconid: (0) taller; (1) subequal; (2) shorter molars other than the first considered when available.
49. Lower molars: talonid: (0) small heel; (1) multicuspidated basin.
50. Lower molars: talonid width relative to trigonid: (0) very narrow, subequal to base of metaconid, developed lingually; (1) narrower; (2) subequal to wider.
51. Lower molars: cristid obliqua: (0) incomplete, with distal metacristid present; (1) complete, attaching below notch in metacristid; (2) complete, labially placed, at base of protoconid.
52. Lower molars: hypoconulid: (0) absent; (1) in posteromedial position; (2) lingually placed and "twinned" with entoconid.
53. Lower molars: entoconid: (0) absent; (1) smaller than hypoconid and/or hypoconulid; (2) subequal to larger than hypoconid and/or hypoconulid.
54. Lower molars: labial postcingulid: (0) absent; (1) present.
55. Ultimate lower molar: hypoconulid: (0) absent; (1) short and erect; (2) tall and sharply recurved.
56. Ultimate lower molar: size relative to penultimate lower molar: (0) subequal; (1) smaller or lost.
57. Space between ultimate lower molar and coronoid process: (0) present; (1) absent.
58. Masseteric fossa: (0) restricted ventrally by crest reaching condyle; (1) extended ventrally to lower margin of dentary.
59. Posterior shelf of masseteric fossa: (0) absent; (1) present.
60. Convex ventral margin behind tooth row continuous to condyle: (0) absent; (1) present.
61. Condyle shape: (0) ovoid; (1) cylindrical.
62. Lower jaw angle: (0) posteriorly directed; (1) medially inflected; (2) posteroventrally directed.
63. Meckelian groove: (0) present; (1) absent.
64. "Coronoid" facet: (0) present; (1) absent.
65. Two large mental foramen, one under second and third premolar and the other under first and second molar: (0) absent; (1) present.

66. Premaxilla: palatal process: (0) does not reach nearly or to canine alveolus; (1) does reach nearly or to canine alveolus.
67. Lateral margin of paracanine fossa: (0) formed by maxilla; (1) maxilla and premaxilla.
68. Zygomatic arch: (0) stout; (1) delicate.
69. Palatal vacuities: (0) absent; (1) present.
70. Palatal expansion behind last molar: (0) absent; (1) present.
71. Minor palatine (postpalatine) foramen: (0) small; (1) large, with thin, posterior bony bridge.
72. Orbitotemporal canal: (0) present; (1) absent.
73. Transverse canal: (0) absent; (1) present.
74. Glenoid fossa shape: (0) concave, open anteriorly; (1) trough-like.
75. Glenoid process of alisphenoid: (0) absent; (1) present.
76. Alisphenoid tympanic process: (0) absent; (1) present.
77. Epitympanic wing medial to promontorium: (0) absent; (1) flat; (2) undulated.
78. Tympanic aperture of hiatus Fallopii: (0) in roof through petrosal; (1) at anterior edge of petrosal; (2) absent.
79. Prootic canal: (0) long and vertical; (1) short and vertical; (2) short and horizontal; (3) absent.
80. Position of sulcus for anterior distributary of transverse sinus relative to subarcuate fossa: (0) anterolateral; (1) posterolateral.
81. Lateral flange: (0) parallels length of promontorium; (1) restricted to posterolateral corner; (2) greatly reduced or absent.
82. Stapedial ratio: (0) rounded, less than 1.8; (1) elliptical, more than 1.8.
83. Complete wall separating cavum supracochleare from cavum epiptericum: (0) absent; (1) present.
84. Caudal tympanic process of petrosal development: (0) tall wall behind postpromontorial recess; (1) tall wall decreasing in height markedly medially; (2) notched between stylomastoid notch and jugular foramen.
85. Rear margin of auditory region: (0) marked by a steep wall; (1) extended onto a flat surface.
86. Stapedius fossa: (0) twice the size of fenestra vestibuli; (1) small and shallow.
87. Hypotympanic sinus: (0) absent; (1) present.
88. Medial process of squamosal in tympanic cavity: (0) absent; (1) present.
89. Posttemporal canal: (0) large; (1) small; (2) absent.
90. Foramen for ramus superior of stapedial artery: (0) present; (1) absent.
91. Transpromontorial sulcus: (0) present; (1) absent.
92. Sulcus for stapedial artery: (0) present; (1) absent.
93. Deep groove for internal carotid artery excavated on anterior pole of promontorium: (0) absent; (1) present.
94. Jugular foramen size relative to fenestra cochleae: (0) subequal; (1) larger.
95. Jugular foramen: (0) confluent with opening for inferior petrosal sinus; (1) separated from opening for inferior petrosal sinus.
96. Inferior petrosal sinus: (0) intrapetrosal; (1) between petrosal, basisphenoid.
97. Ascending canal: (0) present; (1) absent.

Appendix 2

Taxon-character matrix

Amphitherium
000?000?????100?00000?0000100000000000??000000002
00000001100000000???000?????????????????????????

Peramus
0001200?1000000120000000100000000000000000100000
0000100100000?2001??????????????????????????????

Vincelestes
120021010000000022000100210000110111110110100000
100010011110000100000000000000000000000000000000
000

Kielantherium
0???100?????101?111002211000121021111????????0001
00100110?????000?????????????????????????????

Potamotelses
????00?????10122000021010100210221111???????0011
1011011??????????????????????????????????????

Pappotherium
????00?????110100001220101002112111100??????1011
10110??????????0??????????????????????????????

Atokatheridium
???????????111?000002111010021121111????????1001
10100??

Holoclemensia
??01200???00110210011121101002113111110?????1112
1111101??

Oklatheridium
?????0??????110?000002211000121121111????????100?
?0???

Deltatheridium
120010211000110100000221100012112111111111100000
0100110111100111111100001??10?12212010000?111100
111

Deltatheroides
1200102?100011010000022110001211211111111?100000
01001101111????11110????????????????????????????

Sulestes
1200102?1?0?110100000221100012112111111111110000
0100110111100110111?1?0????????22?201??0????110??11

GurilinTsavSkull
120010211000111100000222200012122111100????????
??????????????????11011?10101????2???0?1??????????

Montanalestes

??0?200?????????????????????????????????????01001111
1020000001101????????????????????????????????
Kokopellia
1200101?????111?20000221101002223?211???01100101
1211212001????01?????????????????????????????????
Pariadens
????102?????0121000112221010122131211????????1101
2122110???
Anchistodelphis
1???101?????11110001122220100222322110???????1021
2122120???
Iugomortiferum
?????11?????001?2000022210100222322211????????1021
2122110???
Iqualadelphis
120?101?????11220000122111100222322110?????00100
11122120???
Didelphodon
1212102?10001121202012222010121242211001?1100
21012222110011111111??01????10?2121201101101111
0?101
Eodelphis
12121021100011212020022220101212322110011110021
012122110011111111??01????10?????????0?1?1????????
Pediomys-petrosalA
1200101??00011200001222220100222422110 0??11001021
22221100111?1111??01111????21212011?01?11110?111
Albertatherium
????101?????1111000112221110022232211 00??????1121
21221???
Alphadon
1200101?10001111000112221110022232211 0?00100010
212122110011011111??01????????????????????????????
Turgidodon
1210111??000111100011222101002223221 10???1?00102
121221?00????????????????????121201?001?111100?11
Glasbius
1200110??0001111000122222101002224222101??1110112
122221111?????111???????????????????????????????
Asiatherium
1202101?10001110100022211010022231221 00???00010
212222110010001111???111?11?12????0?10?1???1??????
Mayulestes
120010101000111110001222220101212321110001110010
1112211200??????1110011?0110113?20?00111??1111111
Pucadelphys
12001010100011101021121221110212422110001110011
21222212001101111110001110110112120100101?11111
111
Andinodelphys
12001010100011100021122222111021232211000 11?0011
2122211200110?1?1?10011?11110112?20?00?01?111111
?1

Jaskhadelphys
?????01?????1111002112221111121132211 0??????????
???
Prokennalestes
0001200?010111100100112010000221311110000000010
2110110200000?2001?0?0??0????10101002000?100000?
00
Bobolestes
0001200?????111?1110022010000222311111000101110 2
111110200?00??001????????????????????????????????
Asioryctes
11012000021111301010022010000222312110000000020
21111102000000211100100100000103?211210002?1000
010
Kennalestes
1101200?021111301110022010000222312210010000020
2111110200000?21110010010?0001?30211210002?1000
010
Zalambdalestes
11012001021111322010021110100222312110110100221
212221101000000011100100100000113021121000101000
010
Aspanlestes
0001200?010111300110021110100222322210000 0?1121
212111010000002111?0?????????1020101??0??10110??
10

Appendix 3

List of synapomorehies

Only unambiguously optimized characters are listed. Numbers of nodes corresponds to those in Fig. 8. For the list of characters see Appendix 1.

Node 1: 5(2), 17(2), 25(1), 27(0), 42(1), 48(0), 52(1), 55(1).
Peramus: 4(1), 9(1), 56(0), 62(2), 65(1).
Node 2 (**98**): 2(2), 30(1), 31(1), 33(1), 34(1), 35(1), 36(1), 37(1).
Vincelestes: 6(1), 21(1), 24(2), 39(1), 48(1), 58(1).
Node 3 (**87**): 15(1), 22(2), 30(2), 33(2), 49(1).
Kielantherium: 5(1), 17(1), 18(1), 19(1), 23(2), 29(1).
Node 4 (**51**): 27(1), 50(1).
Potamotelses: 34(2), 38(1), 48(1).
Node 5: 14(1), 17(0), 32(1).
Node 6: 15(0), 23(2).
Pappotherium: 21(1), 48(1).
Node 7: 51(1), 65(1).
Montanalestes: 55(2).
Node 8: 64(1).
Node 9: 4(1), 45(1).
Holoclemensia: 16(2), 20(1), 21(1), 22(1), 38(1).
Node 10 [Eutheria]: 12(1), 15(3), 19(1), 31(2), 32(2).
Node 11; 2(0), 18(1), 81(1).

Node 12: 15(1), 24(0), 27(0), 55(2), 63(0), 64(0).
Prokennalestes: 19(0), 21(1), 22(1), 32(1), 45(0), 51(0).
Bobolestes: 17(1), 38(1).
Aspanlestes: 23(1), 34(2), 36(2), 50(2), 92(1).
Node 13 (**86**): 10(2), 11(1), 79(3), 82(1), 85(1).
Node 14 (**84**): 24(1), 27(0), 45(0), 55(2), 89(2).
Kennalestes: 18(1), 36(2).
Zalambdalestes: 16(2), 17(2), 23(1), 39(1), 45(2), 50(2), 51(2), 62(0), 78(1).
Node 15 [Metatheria]: 5(1), 9(1), 29(1), 41(1), 58(1), 61(1), 66(1), 74(1), 80(1), 90(1), 92(1), 95(1), 97(1).
Node 16 [Deltatheroida, = Deltatheridiidae]: 27(0), 51(0).
Node 17 (**62**): 46(0).
Sulestes: 43(1), 63(0), 67(1).
Node 18: 15(1), 24(2), 32(2), 43(1), 52(20, 54(1), 59(1), 70(1).
Node 19 [Boreometatheria]: 69(1), 76(1).
Guriliin Tsav Skull: 7(2), 27(0).
Node 20: 29(0), 31(2), 35(2).
Node 21: 24(1), 41(0).
Iugomortiferum: 6(1), 13(0), 14(0), 17(2).
Kokopellia: 17(2), 48(1), 52(1), 55(2), 63(0).
Node 22: 43(0).
Asiatherium: 4(2), 16(0), 17(1), 21(2), 34(1), 36(2), 51(2), 59(0), 61(0).
Node 23: 26(1).
Iqualadelphis: 15(2), 16(2), 48(0), 50(1), 55(2).
Node 24: 20(1).
Albertatherium: 47(1).
Node 25: 20(1), 21(10, 60(1).
Node 26: 7(2), 15(2), 29(1), 47(1), 48(0).
Anchistodelphis: 25(2), 55(2).
Turgidodon: 6(1).
Pariadens: 13(0), 32(1), 34(1).
Node 27 (**92**): 17(2), 19(2), 20(0), 25(2), 31(1), 46(2).
Didelphodon: 33(4), 51(2).
Eodelphis: 21(0).
Node 28: 21(2), 33(4), 51(2).
Pediomys: 15(2), 16(0), 25(2).
Glasbius: 6(1), 7(0), 36(2), 39(1), 44(1), 47(1), 56(1), 57(1).
Node 29 [Notometatheria]: 8(0), 21(1), 51(2), 55(2), 75(1), 86(1), 88(1), 93(1), 94(1).
Mayulestes: 17(1), 79(3).
Node 30 (**68**): 19(2), 20(1), 26(1), 28(1), 35(2).
Jaskhadelphys: 32(1).
Node 31 (**80**): 16(0), 29(0).
Pucadelphys: 17(1), 23(1), 33(4), 53(2).
Andinodelphys: 69(1), 73(1).

Appendix 4

List of changes from the matrix of Rougier et al. (1998, 2004)

Amphitherium: 3(?), 8(?), 9(?), 10(?), 12(?), 13(?), 14(?), 15(1), 16(0), 20(0), 21(0), 24(0), 26(0), 29(0), 30(1), 31(0), 33(NA), 34(NA), 37(NA), 38(NA), 39(NA), 41(?), 53(NA), 58(0), 61(1), 64(?), 65(?), 66(?), 70(1), 76(0), 77(0), 78(?), 79(?), 80(?), 81(?), 82(?), 83(?), 84(?), 85(?), 86(?), 87(?), 88(?), 89(?).

Peramus: 14(0), 16(0), 33(NA), 34(NA), 37(NA), 38(NA), 39(NA), 42(0), 46(0), 47(0), 58(0), and 70(1).

Kielantherium: 1(?), 15(1), 16(0), 17(1), 20(1), 21(1), 22(1), 23(0), 24(0), 25(2), 26(2), 27(1), 28(1), 29(0), 30(0), 31(0), 33(1), 34(0), 35(0), 36(2), 37(0), 38(0), 39(0), 40(1), 45(?), 47(?).

Holoclemensia: 2(0), 3(1), 4(2), 6(0), 13(0), 14(0), 33(1), 47(1), 53(0).

Pappotherium: 6(0), 19(1), 33(1), 36(2), 41(0), 48(1), 51(0), 57(1), 58(0), 77(0).

Potamotelses: 4(?), 15(0&1), and 33(1).

Montanalestes: 2(0), 4(2), 5(0), 6(0), 47(0), 48(1), 49(1), 50(1), 51(1), 52(1), 53(1), 54(1), 55(0), 56(0), 57(0), 58(0), 59(0), 60(0), 61(0), 63(0), 67(0), 68(0), 69(0), 70(0), 72(1), 73(1), 74(1), 75(1), 76(0), 77(1).

Kokopellia: 75(0).

Sulestes: 1(2), 2(0), 3(0), 4(1), 7(1), 10(1), 11(0), 13(0), 18(1), 24(0), 41(1), 42(1), 43(1), 44(1), 45(1), 46(0), 47(0), 53(0), 61(1), 62(1), 63(1), 67(1), 68(0), 69(0), 70(1), 71(1), 72(0), 73(1), 74(1), 75(0&1), 76(1), 77(1), 81(1), 82(1), 83(0), 93(0), 123(2), 124(2), 126(2), 127(0), 128(1), 129(1), 133(0), 137(0), 139(0), 146(1), 147(1), 148(0), 151(1), 152(2), 153(0).

Guriliin Tsav: 11(0), 20(0), 22(0), 30(0), 36(2), 38(0), 95(?), 97(?), and 99(0).

Prokennalestes: 10(0), 11(1), 43(0), 45(0).

Bobolestes: 3(?), 17(1), 18(1), 19(?), 20(1), 21(1), 37(0), 38(0), 41(0), 42(0), 43(0), 46(1), 70(1), 72(0), 73(?), 77(1).

Asioryctes: 11(1), 44(0) and 59(0).

Kennalestes: 11(1).

Aspanlestes: 10(0), 11(1), 19(0), 44(?), 46(1), 53(0), 62(0), 70(0), 71(0), 74(1), 75(1), 76(1), 122(1), 123(0), 124(2), 125(0), 126(1), 127(0), 128(1), 129(1), 133(0), 134(0), 139(0), 144(1), 145(0), 146(1), 147(1), 148(0), 151(1), 152(0), 153(0).